

Statistics of planar graphs viewed from a vertex: A study via labeled trees

J. Bouttier¹, P. Di Francesco² and E. Guitter³

Service de Physique Théorique, CEA/DSM/SPhT

Unité de recherche associée au CNRS

CEA/Saclay

91191 Gif sur Yvette Cedex, France

We study the statistics of edges and vertices in the vicinity of a reference vertex (origin) within random planar quadrangulations and Eulerian triangulations. Exact generating functions are obtained for these graphs with fixed numbers of edges and vertices at given geodesic distances from the origin. Our analysis relies on bijections with labeled trees, in which the labels encode the information on the geodesic distance from the origin. In the case of infinitely large graphs, we give in particular explicit formulas for the probabilities that the origin have given numbers of neighboring edges and/or vertices, as well as explicit values for the corresponding moments.

07/03

¹ bouttier@spht.saclay.cea.fr

² philippe@spht.saclay.cea.fr

³ guitter@spht.saclay.cea.fr

1. Introduction

The study of random planar graphs is a subject of interest in several areas of physics, ranging from two-dimensional quantum gravity, where planar graphs provide a natural discretization of space-time, to soft condensed matter where they can be used for instance to model fluid membranes. By random planar graphs, we mean here graphs embedded in the plane (or in the two-dimensional sphere), also referred to as fatgraphs in the physics literature or maps in mathematics.

The statistical properties of random planar graphs have been studied by various techniques over the years. Beside the original combinatorial method due to Tutte [1], and the quite technical matrix integral formulation [2-4], the most recent approach consists in a bijective enumeration [5], based on a one-to-one correspondence between planar graphs and suitably decorated trees, whose statistics is easily characterized by recursive relations. Apart from its simplicity, one of the advantages of the bijective approach is that it naturally keeps track of the distances between vertices on the graphs. This property was used in particular in Ref.[6] to derive the statistical distribution for the so-called radius of quadrangulations, and in Ref.[7] to obtain the distribution of distances between two vertices in graphs made of even-sided polygons. It also gives access to a more refined study of the *local environment* of a vertex in random graphs, through the statistics of its number of nearest, next-nearest, ... neighbors.

The purpose of this paper is precisely to use the bijective approach to derive the probability for a given vertex to have a number, say n_i , of neighboring vertices and/or a number, say m_i , of neighboring edges at a finite distance i . The case of nearest neighbors was already addressed in Ref.[8] for the particular case of planar triangulations with no multiple edges and no loops. In this particular case, a vertex with k neighbors may be replaced by a face with k sides, which makes the problem accessible to standard matrix integral techniques. This approach however breaks down for graphs with multiple edges or loops and is limited to the immediate neighbors.

In this paper, we consider the case of both quadrangulations and Eulerian (i.e. face bi-colored) triangulations. In the former case, our analysis relies on a bijection described in Ref.[6] between rooted planar quadrangulations and so-called well-labeled trees, i.e. rooted planar trees with vertices labeled by non-negative integers, with a root vertex labeled 1 and with the constraint that labels on adjacent vertices on the tree differ by at most 1. In the latter case, a similar bijection will be derived below between rooted planar Eulerian

triangulations and a more restricted class of well-labeled trees where the labels on adjacent vertices are required to differ by *exactly* 1.

The paper is organized as follows. In Section 2, we present the correspondences between quadrangulations or Eulerian triangulations on one hand, and well-labeled trees on the other hand. In Section 3, we first recall known enumeration results for well-labeled trees (Sect.3.1), and then show how to extract the statistics of vertices and/or edges at distance i from a given vertex by computing generating functions for suitably weighted well-labeled trees (Sect.3.2). When restricting to the case of the local environment (i.e. finite distances), we extend our study to the limiting case of infinitely large graphs (Sect.3.3). The following sections (4,5,6) are devoted to a detailed study of nearest neighbor statistics. In Section 4, we obtain algebraic equations for the associated generating function, which we use in Section 5 to calculate various probabilities and moments. Section 6 presents a heuristic interpretation of our results in the form of a phase diagram for a statistical model of embedded trees. We complete our study by presenting in Section 7 a shortcut to treat the general case of more distant neighbors. We gather a few concluding remarks in Section 8.

2. Geodesic distance in planar graphs: From graphs to well-labeled trees

In this section, we first recall the construction of Ref.[6] establishing a bijection between on one hand rooted planar *quadrangulations* and on the other hand well-labeled trees, as defined above. This construction uses crucially the notion of geodesic distance between vertices in the quadrangulation and allows for an easy characterization of the number of neighbors of a given vertex. We then show how to adapt this construction to establish a bijection now between rooted planar *Eulerian triangulations* and a slightly different class of well-labeled trees.

2.1. Quadrangulations

Let us start with a rooted planar quadrangulation, i.e a planar map with all its faces of valence four (i.e. having four sides) and with a marked edge bordering the infinite face and oriented clockwise around the quadrangulation. The *origin* of the quadrangulation is the vertex from which the marked edge originates. For each vertex, we define its geodesic distance from the origin as the minimal number of edges of the paths linking the origin to this vertex. We may then label each vertex by its geodesic distance from the origin.

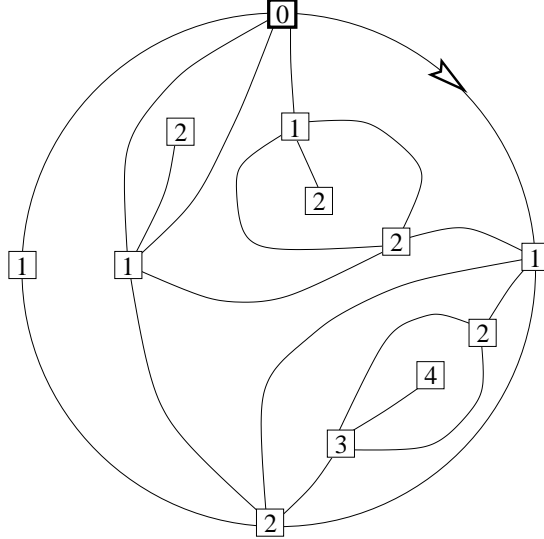


Fig.1: A sample rooted planar quadrangulation. An unambiguous representation in the plane is obtained by having the marked edge adjacent to the external face and oriented clockwise around the graph. Each vertex is labeled by its geodesic distance from the origin of the marked edge (labeled 0).

With this labeling, the origin is the only vertex labeled by 0, while all other vertices have positive labels. In particular, the nearest neighbors of the origin are the vertices labeled by 1 (see Fig.1).

Each face of the quadrangulation may be classified, upon reading the four labels of the vertices around it in clockwise direction, in one of the two following categories (see Fig.2) :

- (i) “simple” faces with a sequence of labels of the form $n \rightarrow n + 1 \rightarrow n + 2 \rightarrow n + 1$
- (ii) “confluent” faces with a sequence of labels of the form $n \rightarrow n + 1 \rightarrow n \rightarrow n + 1$

Indeed, neighboring vertices have labels which differ by at most one by construction and the bipartite nature of the quadrangulation implies that the parity of the labels changes from any vertex to its neighbor. We now build a well-labeled tree with rules resulting from the above classification (see Fig.2):

- (i) For each simple face, we retain the edge $n + 1 \rightarrow n + 2$ (in clockwise direction ⁴)
- (ii) For each confluent face, we draw a new edge linking the two vertices with labels $n + 1$

The object resulting from the collection of these edges is a planar graph whose vertices are vertices of the original quadrangulation. Let us now show that it is indeed a well-labeled

⁴ Here and throughout the paper, when we work in the planar representation, the rule must be reversed for the external face, i.e. the labels are to be read in *counterclockwise* direction around the graph.

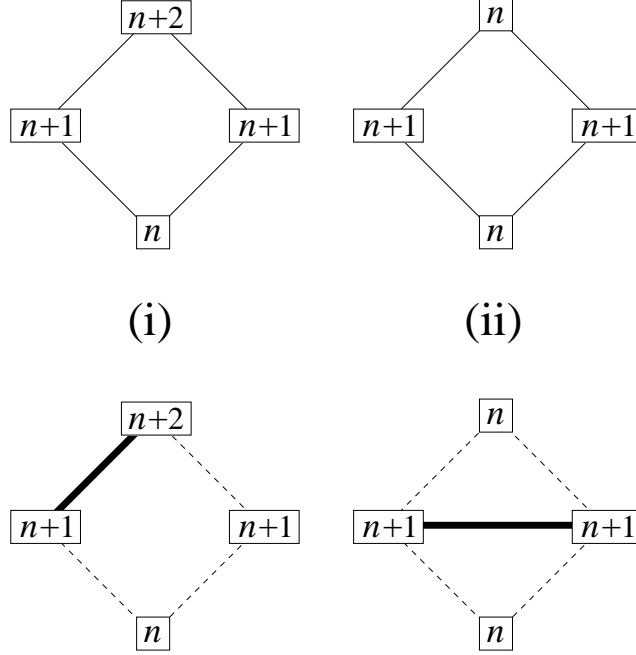


Fig.2: The two possible configurations of labels around a face in a quadrangulation: (i) a simple face and (ii) a confluent face. To each face is associated an edge (thick solid line) as indicated below. The collection of these edges will eventually produce the well-labeled tree associated to the original quadrangulation.

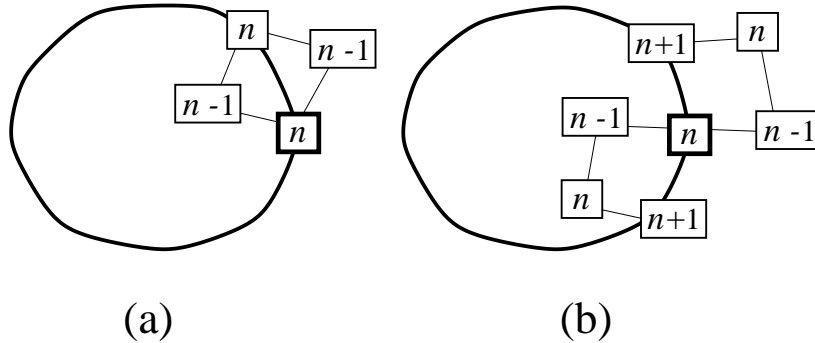


Fig.3: The impossibility of loops in the collections of edges as built from the rules of Fig.2. Indeed, such a loop would have a vertex with minimal label n whose environment would be either (a) or (b). In both cases, a vertex of label $n - 1$ is present on both sides of the loop, which contradicts the definition of labels as geodesic distances from the origin.

tree. Let N denote the number of faces of the original quadrangulation, with therefore $2N$ edges and $N + 2$ vertices. We note that N is also the number of edges of the graph resulting from the above construction as each face produces an edge and the resulting edges are all distinct (this is clear for confluent faces and results from the orientation prescription

for simple faces). It is now sufficient to prove that the graph contains no loop. Suppose that such a loop exists, we pick a vertex with a minimal label, say n , along this loop. By examining all possible configurations (see Fig.3), we see that this vertex is adjacent to at least one vertex labeled $n - 1$ on each side of the loop. This is a contradiction as the labels represent the geodesic distance: among the geodesic paths linking the origin to these vertices, one must cross the loop at a vertex with label less than $n - 1$, in conflict with the property that all labels on the loop are larger than n . The graph is therefore made of $C \geq 1$ connected planar trees, hence has $N + C$ vertices. On the other hand, the number of vertices is at most $N + 1$ as the origin cannot belong to a retained edge. We deduce that $C = 1$, hence the graph is a connected tree containing all the vertices of the quadrangulation but the origin. This tree is well-labeled as all labels are positive and labels on adjacent vertices differ by at most one by construction.

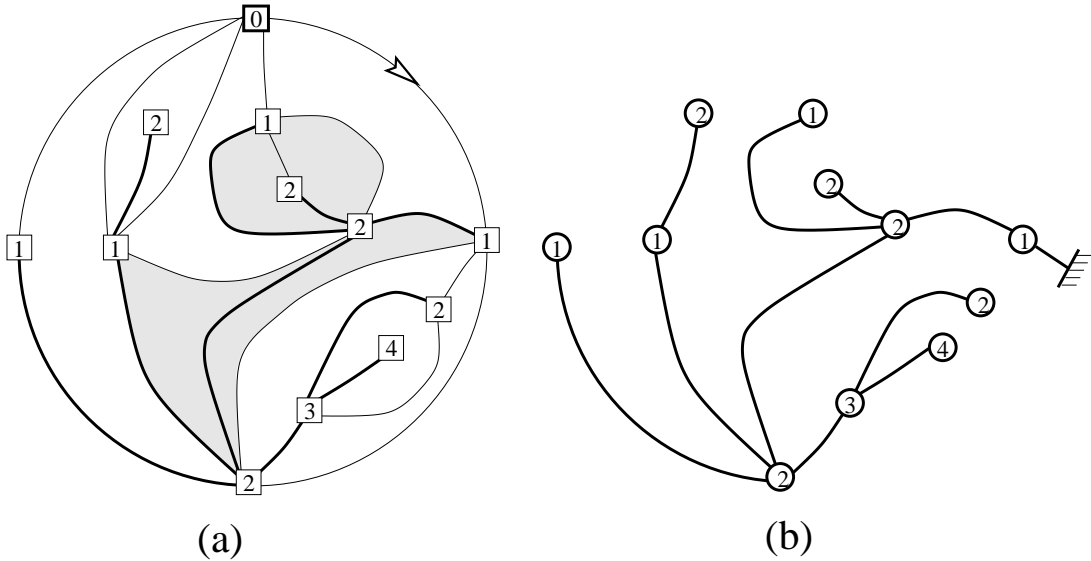


Fig.4: The construction of the well-labeled tree associated with the rooted quadrangulation of Fig.1: the edges selected (a) according to the rules of Fig.2 produce the well-labeled tree (b). The tree is rooted at the vertex (labeled 1) where the original marked edge ends. We have shaded the confluent faces in (a).

The tree is naturally rooted according to the position of the marked edge in the original rooted quadrangulation (see Fig.4)

So far we have associated to each rooted planar quadrangulation a rooted planar well-labeled tree. Let us now describe the inverse procedure. Starting from a well-labeled tree, we restore an origin by adding an extra vertex labeled 0. Non-intersecting edges are added

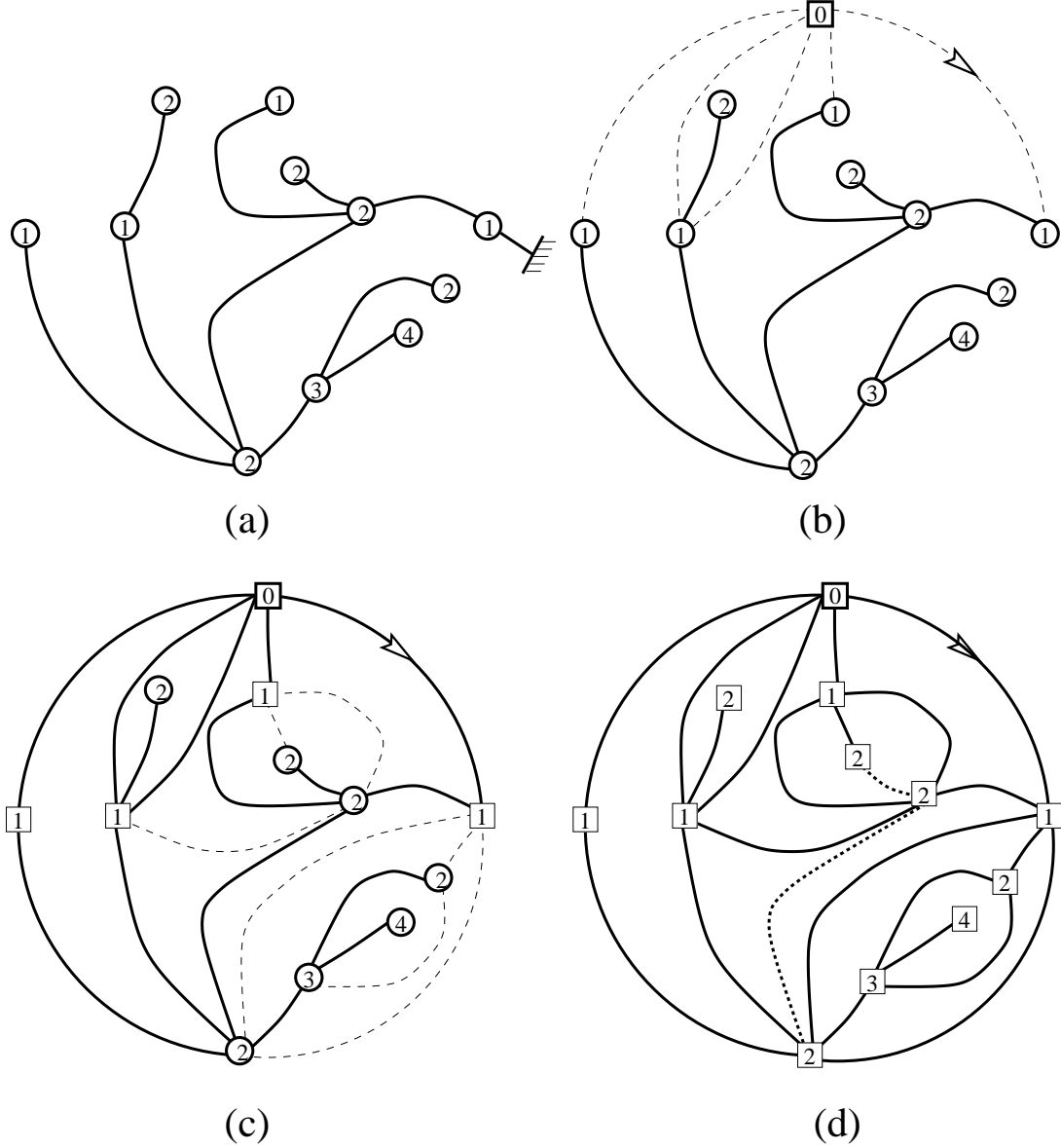


Fig.5: The inverse construction of Fig.4 from the well-labeled tree (a) to the quadrangulation of Fig.1. We first restore the origin and connect it to each corner at all vertices labeled 1 (b). Within each of the newly created faces, further connections are made according to the rules explained in the text (c). The final step is to remove all edges connecting vertices with equal labels (d).

between this vertex and each vertex labeled 1 with one connection per *corner* at this vertex (see Fig.5). The position of the root of the tree naturally translates into a marking of one of these newly created edges. The resulting map is made of a number of faces in which we apply the following construction independently. Reading the labels of the corners (as inherited from the label of the adjacent vertex) in clockwise direction around the face, we connect by a new edge each corner with label $n \geq 2$ to the first encountered corner with

label $n - 1$, unless this latter corner is the immediate successor of the former and in such a way that the added edges do not cross each other. Finally, a planar rooted quadrangulation is obtained by erasing all the edges linking vertices with identical labels. We rely on Ref.[6] for a formal proof that the above constructions are inverse of one-another.

This bijection between rooted planar quadrangulations and well-labeled trees keeps track of the local environment of the origin. For instance, the vertices labeled 1 in the tree are the nearest neighbors of the origin, those labeled 2 the next-nearest neighbors and so on. This allows in particular to count the number of nearest neighbors of the origin as the number of vertices labeled 1 in the tree. Note that this number *does not* account for the multiplicity of the neighbors, which are all counted once even if they are connected by several edges to the origin. The number of nearest neighbors counted with their multiplicity is nothing but that of edges connected to the origin. In the language of well-labeled trees, this is the total number of corners labeled 1, or equivalently the sum of the valences of all vertices labeled 1.

2.2. Eulerian triangulations

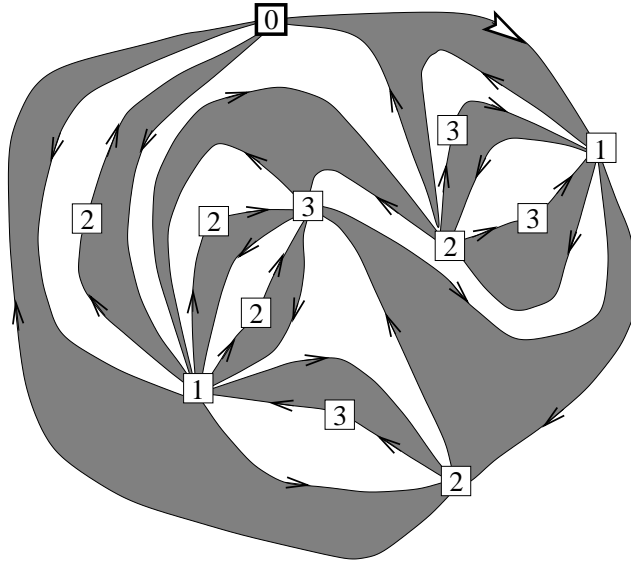


Fig.6: A sample rooted planar Eulerian (face-bicolored) triangulation. An unambiguous representation in the plane is obtained by having the marked edge adjacent to the external face and oriented clockwise around the graph. This orientation induces an orientation of all the other edges as shown. Each vertex is labeled by its geodesic distance from the origin of the marked edge (labeled 0). This distance is now defined with paths respecting the orientation.

We now intend to adapt the above constructions to the case of planar *Eulerian* triangulations, i.e. planar maps with all faces of valence three (hereafter referred to as triangles) and with an even number of triangles around each vertex (see Fig.6). These triangulations are equivalently characterized by the property that their faces are bicolorable or that their vertices are tricolorable [9].

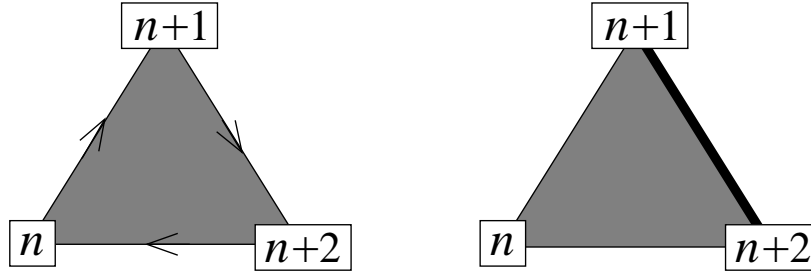


Fig.7: The configuration of labels around a clockwise oriented (black) face in an Eulerian triangulation. To each black face is associated an edge (thick solid line) as indicated on the right. The collection of these edges will eventually produce the well-labeled tree associated to the original Eulerian triangulation.

We start from a rooted such triangulation, with a marked edge bordering the infinite face and oriented clockwise around the triangulation. This fixes a natural orientation for every edge by requiring that orientations alternate around each vertex. This in turn gives a natural bicoloration of the faces in say black and white according to the clockwise or counterclockwise orientation of the adjacent edges. Taking as before for origin the vertex from which the marked edge originates, we define the geodesic distance of any vertex from the origin as the minimal number of edges of the paths linking the origin to that vertex and *respecting the orientations*. This defines a labeling of the vertices, such that the sequence of labels around all clockwise oriented (black) faces is of the form $n \rightarrow n + 1 \rightarrow n + 2$ (see Fig.7). This follows from the fact that neighboring vertices have labels which differ by at most two while the tricolorability of the vertices fixes the residue modulo 3 of all labels. We now build a well-labeled tree by a similar rule as for quadrangulations by retaining for each clockwise oriented (black) face with labels say $n \rightarrow n + 1 \rightarrow n + 2$ the edge linking the vertices labeled $n + 1$ and $n + 2$ (see Fig.7).

The resulting object is a well-labeled tree with the stronger constraint that adjacent vertices have labels differing by *exactly* 1. To see that, we follow the same line of reasoning as above. Let N denote the number of black faces of the triangulations with therefore $2N$ faces, $3N$ edges and $N + 2$ vertices. The graph resulting from the above construction has

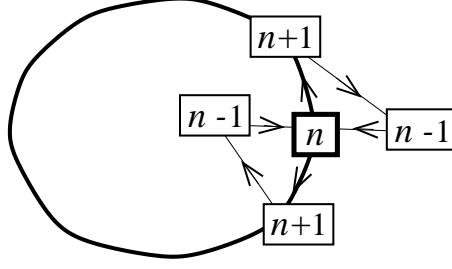


Fig.8: The impossibility of loops in the collections of edges as built from the rules of Fig.7. Indeed, such a loop would have a vertex with minimal label n which would be adjacent to a vertex labeled $n - 1$ on both sides of the loop, which contradicts the definition of labels as geodesic distances from the origin.

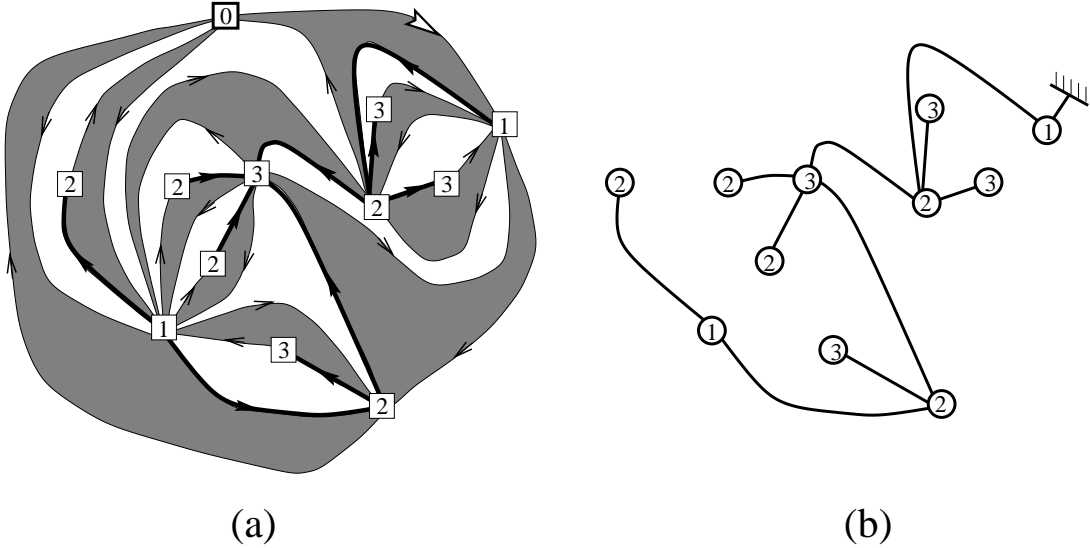


Fig.9: The construction of the well-labeled tree associated with the rooted Eulerian triangulation of Fig.6: the edges selected (a) according to the rules of Fig.7 build the well-labeled tree (b)

N edges and contains no loop (see Fig.8). It is therefore made of C connected trees and $C = 1$ since the total number of vertices $N + C$ is less than $N + 1$ as the origin does not belong to any selected edge.

The tree is naturally rooted according to the position of the marked edge in the original rooted Eulerian triangulation (see Fig.9)

Let us now describe the inverse construction, which consists in iteratively building the black clockwise-oriented triangles. Starting from a rooted well-labeled tree with adjacent labels differing by exactly one, we construct the associated Eulerian triangulation step by step as follows. The step 0 consists in adding an origin and linking it to the right of

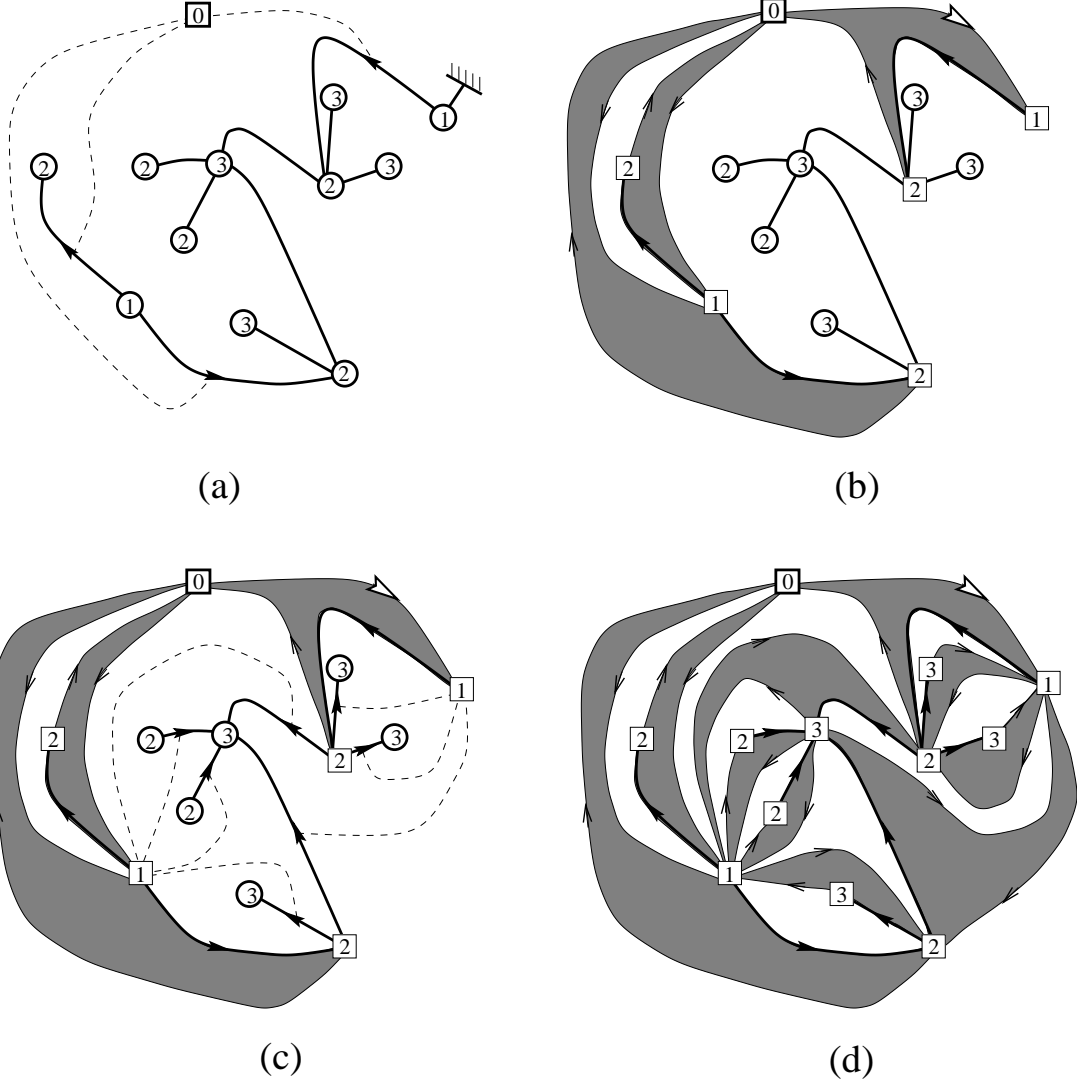


Fig.10: The inverse construction of Fig.9. Starting from the well-labeled tree, we first restore the origin and link it to the right of each $1 \rightarrow 2$ edge (a). The links are then inflated into $0 \rightarrow 1 \rightarrow 2$ black triangles (b). We proceed within each of the newly created white faces by linking the unique vertex labeled 1 within the face to the right of the $2 \rightarrow 3$ edges (c). These links are inflated into $1 \rightarrow 2 \rightarrow 3$ black triangles. The procedure is repeated until an Eulerian triangulation is obtained, which is already the case here (d).

each edge with labels 1 and 2, oriented from 1 to 2. Each such link is inflated so as to create a clockwise oriented (black) triangle $0 \rightarrow 1 \rightarrow 2$. Beside these triangles, the original external face is split into a number of white faces (see Fig.10). It is easily seen that the sequence of labels in clockwise orientation around any of these white faces is of the form $0 \rightarrow 2 \rightarrow \dots \rightarrow 2 \rightarrow 1$ where all labels in-between the first and the last 2-labels are greater or equal to 2 and all increments but the first ($0 \rightarrow 2$) are ± 1 . In particular, if the sequence

is reduced to $0 \rightarrow 2 \rightarrow 1$, a white triangle has been created. We then proceed to the step 1 which takes place independently inside each white face not reduced to a triangle. For a given such face F , each $2 \rightarrow 3$ edge having its right side adjacent to F is linked from this side to the unique vertex labeled 1 around F . As before, we inflate this link, thus creating a black triangle $1 \rightarrow 2 \rightarrow 3$. As F is not reduced to a triangle, it is easy to see that at least one black triangle is created. Beside these additional black faces, the face F is split into smaller white faces. Among these faces, that containing the origin is a triangle $0 \rightarrow 2 \rightarrow 1$ and the others of the form $1 \rightarrow 3 \rightarrow \dots \rightarrow 3 \rightarrow 2$ such that all labels in-between the first and the last 3-labels are greater or equal to 3, and all increments but the first ($1 \rightarrow 3$) are ± 1 . These faces, if not reduced to triangles, have to be split again by repeating the above procedure. At step i , all faces are either black or white triangles or larger white faces of the form $i \rightarrow i+2 \rightarrow \dots \rightarrow i+2 \rightarrow i+1$ where all labels in-between the first and the last $i+2$ -labels are greater or equal to $i+2$ and all increments but the first ($i \rightarrow i+2$) are ± 1 . The procedure ends when all labels are exhausted and leaves us with an Eulerian triangulation rooted at the $0 \rightarrow 1$ edge linking the origin to the root of the original tree.

Let us now finally show that the two constructions above, respectively from an Eulerian triangulation to a well-labeled tree and conversely are inverse of one-another. It is straightforward that, starting from a well-labeled tree and building the associated triangulation, the latter is re-decomposed into the same labeled tree as the construction of black triangles always consists in adding edges of the form $n \rightarrow n+1$ and $n+2 \rightarrow n$ to tree-edges of the form $n+1 \rightarrow n+2$. To complete the proof of the bijection it is now sufficient to show that the number of objects is the same within the two classes, namely on one hand rooted planar Eulerian triangulations with N black faces, and on the other hand rooted well-labeled trees with N edges. The former number was first obtained in Ref.[1] with the result $3 \cdot 2^{N-1} (2N)! / (N!(N+2)!)$. The latter number will be derived below and is identical, which completes the proof.

As for the case of quadrangulations, the bijection between Eulerian triangulations and well-labeled trees allows to keep track of the numbers of nearest, next nearest, etc ... neighbors of the origin in Eulerian triangulations. Note that the notion of neighbors now uses the edge orientations. As before, we have access to the number of neighbors both with and without their multiplicity.

3. Planar graphs viewed from a vertex: statistics of neighboring edges and vertices

In this section, we use the above bijections to study the general statistics of edges and vertices at fixed geodesic distances from a given vertex (origin) in arbitrary quadrangulations and Eulerian triangulations. This is done via the enumeration of properly weighted well-labeled trees. We first recall how to perform this enumeration by use of recursion relations in the absence of weights, and then proceed to the weighted case. Finally, in the case of neighbors within a finite range of distances, we show how to derive algebraic equations for the various generating functions at hand.

3.1. Enumeration of well-labeled trees

The above bijections reduce the problem of enumeration of quadrangulations or Eulerian triangulation to that, much simpler, of well-labeled trees. This is done via the computation of their generating functions with a weight g per edge. More precisely, we introduce the generating functions W_j , $j = 1, 2, \dots$, for rooted trees with positive labels and with a root labeled j . In view of the above bijections, the function W_1 is indeed identified with the generating function for rooted quadrangulations (resp. Eulerian triangulations) with a weight g per face (resp. per black face). We are therefore only interested in W_1 , but in practice, the scheme we propose involves the simultaneous computation of all W_j 's. From the constraint that adjacent vertices have labels differing by at most or exactly one, we deduce the following master equations:

$$\begin{aligned} W_j &= \frac{1}{1 - g(W_{j+1} + W_j + W_{j-1})} && \text{(Quadrangulations)} \\ W_j &= \frac{1}{1 - g(W_{j+1} + W_{j-1})} && \text{(Eulerian Triangulations)} \end{aligned} \tag{3.1}$$

obtained by inspection of the descendents of the root vertex (see Ref.[10]). These recursion relations must be supplemented by the boundary condition $W_0 = 0$ and restricted to values of $j = 1, 2, 3, \dots$. The solution is then unique as one readily sees by expanding eqs.(3.1) order by order in g and noting that all W 's are series of g with only non-negative powers by definition.

The explicit solutions of eqs.(3.1) were worked out in Ref.[7], with the results

$$\begin{aligned} W_j &= W \frac{u_j u_{j+3}}{u_{j+1} u_{j+2}} && \text{(Q.)} \\ W_j &= W \frac{u_j u_{j+4}}{u_{j+1} u_{j+3}} && \text{(E.T.)} \end{aligned} \tag{3.2}$$

with

$$\begin{aligned} W &= \frac{1 - \sqrt{1 - 12g}}{6g} & (\text{Q.}) \\ W &= \frac{1 - \sqrt{1 - 8g}}{4g} & (\text{E.T.}) \end{aligned} \tag{3.3}$$

and where

$$u_j = 1 - x^j \quad \text{with} \quad \begin{cases} x = \frac{1+2\theta^2-\theta\sqrt{3(2+\theta^2)}}{1-\theta^2} & \theta = (1-12g)^{\frac{1}{4}} & (\text{Q.}) \\ x = \frac{1-\theta}{1+\theta} & \theta = (1-8g)^{\frac{1}{4}} & (\text{E.T.}) \end{cases} \tag{3.4}$$

In particular, eqs.(3.2) yield the following formulas for W_1 :

$$\begin{aligned} W_1 &= \frac{4(1+2\theta^2)}{3(1+\theta^2)^2} & (\text{Q.}) \\ W_1 &= \frac{5+10\theta^2+\theta^4}{4(1+\theta^2)^2} & (\text{E.T.}) \end{aligned} \tag{3.5}$$

with θ as in eq.(3.4). For Eulerian triangulations, we easily extract from the above formula the number of well-labeled trees with N edges

$$W_1|_{g^N} = 3 \cdot 2^{N-1} \frac{(2N)!}{N!(N+2)!} \tag{3.6}$$

where the subscript $|_{g^N}$ refers to the coefficient of g^N in the corresponding series. This number coincides with the number of rooted planar Eulerian triangulations with $2N$ faces, and allows to complete the proof of the bijection of Sect.2, as announced.

The function W of eq.(3.3) is the limit of W_j for large j . By a global shift of labels, the function W_j may be understood as counting trees with a root labeled 1 and with all labels $\geq 2 - j$. The function W therefore simply counts rooted trees with a root labeled 1 and with possibly negative integer labels. Interestingly enough, the function W may also be interpreted in the language of graphs. In the case of quadrangulations, it is easily identified as the generating function with a marked vertex and a marked edge, while W_1 is the generating function with only a marked oriented edge (here we make use of the spherical representation of planar graphs for simplicity). If Q_N denotes the total number of quadrangulations on the sphere with N faces (counted with their inverse symmetry factor), we have $W|_{g^N} = (N+2)(2N)Q_N$ while $W_1|_{g^N} = 2(2N)Q_N$, hence $W_1|_{g^N} = 2/(N+2)W|_{g^N} = 2 \cdot 3^N c_N / (N+2)$ where $c_N = \binom{2N}{N} / (N+1)$ is the N -th Catalan number, a result already obtained in Ref.[11] via tree conjugacy, and consistent with the solution (3.5), as checked in Ref.[7].

Similarly, in the case of Eulerian triangulations, the function W is identified with the generating function with a marked (origin) vertex and a marked oriented edge of type $j \rightarrow j+1$ with respect to this origin and with a global orientation induced by that of the marked edge, while W_1 is the generating function with a marked oriented edge (here again, we make use of the spherical representation of planar graphs for simplicity). If E_N denotes the total number of oriented Eulerian triangulations on the sphere with $2N$ faces (counted with their inverse symmetry factor), we have $W|_{g^N} = (N+2)(2/3)(3N)E_N$, as for a fixed origin, exactly $2/3$ of the edges will be of type $j \rightarrow j+1$, while $W_1|_{g^N} = (3N)E_N$, hence $W_1|_{g^N} = 3/(2(N+2))W|_{g^N} = 3 \cdot 2^{N-1} c_N / (N+2)$, a result already obtained in Ref.[9] via matrix models and in Ref.[12] via tree conjugacy, and also consistent with the solution (3.6).

3.2. Statistics of edges and vertices at fixed distances from an origin

So far the counting functions have not kept track of the numbers of vertices and edges at a given distance from the origin in the graphs. This can be repaired by considering the same generating functions W_j as before but with extra weights, namely ρ_i per vertex labeled i in the tree, and α_i per edge adjacent to a vertex labeled i (an edge linking a vertex labeled i to a vertex labeled k thus receives the weight $\alpha_i \alpha_k$). From now on, we shall use the shorthand notation $W_j \equiv W_j(\{\alpha_i; \rho_i\})$ for the generating function incorporating all the weights α_i and ρ_i , while the W_j 's of previous section will be written as $W_j(\{1; 1\})$. Taking into account these new weights, the master equations become

$$\begin{aligned} W_j &= \frac{\rho_j}{1 - g\alpha_j(\alpha_{j+1}W_{j+1} + \alpha_j W_j + \alpha_{j-1}W_{j-1})} & (\text{Q.}) \\ W_j &= \frac{\rho_j}{1 - g\alpha_j(\alpha_{j+1}W_{j+1} + \alpha_{j-1}W_{j-1})} & (\text{E.T.}) \end{aligned} \tag{3.7}$$

which, together with $W_0 = 0$, determine again the W 's completely as powers series in g .

Let us now show how to extract from these generating functions the statistics of neighbors in quadrangulations of Eulerian triangulations. The neighbor statistics is entirely characterized by the following average:

$$\begin{aligned} \Gamma_N &\equiv \langle \prod_{j \geq 1} \alpha_j^{m_j} \rho_j^{n_j} \rangle_N = \frac{\Delta_N(\{\alpha_j; \rho_j\})}{\Delta_N(\{1; 1\})} \\ \Delta_N(\{\alpha_j; \rho_j\}) &= \sum_{(\mathcal{G}, v \in \mathcal{G})} \alpha_j^{m_j(\mathcal{G}, v)} \rho_j^{n_j(\mathcal{G}, v)} / |Aut(\mathcal{G}, v)| \end{aligned} \tag{3.8}$$

where the statistical sums extend over all pairs (\mathcal{G}, v) made of a quadrangulation \mathcal{G} (resp. an Eulerian triangulations \mathcal{G}) with N faces (resp. N black faces) on the sphere and a vertex v of \mathcal{G} . Here $n_j(\mathcal{G}, v)$ is the number of vertices at geodesic distance j from the vertex v while $m_j(\mathcal{G}, v)$ denotes the number of edges $(j-1, j)$ linking a vertex at distance $j-1$ from v to a vertex at distance j from v . For instance, $n_1(\mathcal{G}, v)$ (resp. $m_1(\mathcal{G}, v)$) denotes the number of nearest neighboring vertices (resp. edges) of v in \mathcal{G} . The factor $|Aut(\mathcal{G}, v)|$ is the usual symmetry factor of the marked graph on the sphere.

The statistical sum Δ_N is related to W_1 via

$$\alpha_1 \frac{d}{d\alpha_1} \Delta_N(\{\alpha_j; \rho_j\}) = W_1(\{\alpha_j; \rho_j\})|_{g^N} \quad (3.9)$$

The derivation with respect to α_1 amounts to counting the graphs \mathcal{G} (already marked at v) with a multiplicity $m_1(\mathcal{G}, v)$ equal to the number of edges originating from v . This corresponds precisely to counting graphs with a marked oriented edge on the sphere, i.e. *rooted planar maps*.

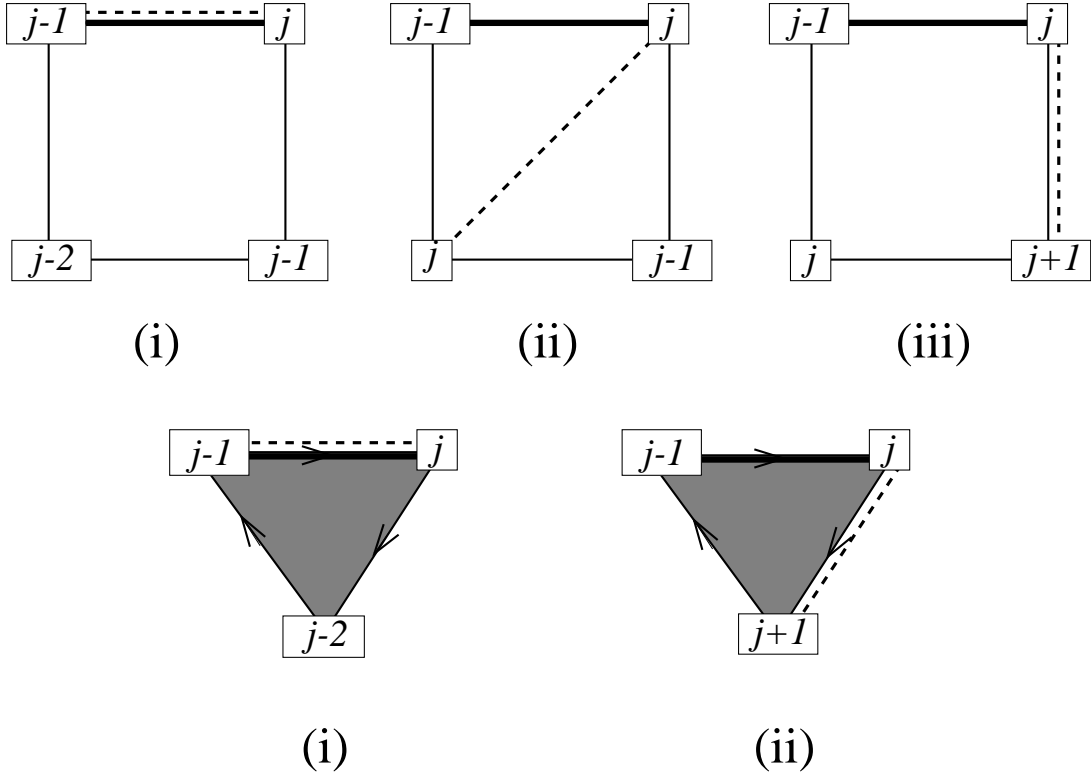


Fig.11: The one-to-one correspondence between $(j-1, j)$ edges (represented in thick lines) in quadrangulations (top) or Eulerian triangulations (bottom) and edges adjacent to vertices labeled j in the corresponding well-labeled trees (dashed lines).

The relation (3.9) follows from the fact that the total number of vertices at geodesic distance j from the origin is equal to that of vertices labeled j in the associated well-labeled trees, while the total number of edges $(j-1, j)$ in the graph is equal to the total number of edges adjacent to a vertex labeled j in the associated well-labeled tree. To see the latter property, note that the face adjacent to the $(j-1, j)$ edge and on its right contains exactly one edge of the tree adjacent to the vertex labeled j in this edge. This is done by inspecting all possible cases for quadrangulations and Eulerian triangulations (see Fig.11). Conversely, to each edge adjacent to a vertex labeled j in the well-labeled tree, say of the form (j, i) , we may associate a unique edge $(j-1, j)$ of the graph. We have indeed the following possibilities for quadrangulations (respectively associated to the three situations of the first line of Fig.11):

- (i) $i = j-1$: the edge (i, j) is the $(j-1, j)$ edge
- (ii) $i = j$: the edge (i, j) is a diagonal of a square $(j-1, j, j-1, j)$, and we pick the edge $(j-1, j)$ on its left
- (iii) $i = j+1$: the edge (j, i) has a square on its right of the form $(j-1, j, j+1, j)$, in which we pick the edge $(j-1, j)$ adjacent to (j, i)

For Eulerian triangulations we only have two possibilities (respectively associated to the two situations of the second line of Fig.11):

- (i) $i = j-1$: the edge (i, j) is the $(j-1, j)$ edge
- (ii) $i = j+1$: the edge (j, i) is adjacent to a black triangle on its right, of the form $(j-1, j, j+1)$, in which we pick the $(j-1, j)$ edge

This completes the bijection between the edges $(j-1, j)$ of the graph and those adjacent to the same vertex labeled j in the tree.

In conclusion, inverting eq.(3.9), the knowledge of W_1 as determined by eqs.(3.7) gives access to the statistical average Γ_N via

$$\Gamma_N = \frac{\int_0^{\alpha_1} \frac{d\alpha}{\alpha} W_1(\{\alpha, \alpha_2, \dots; \rho_1, \rho_2, \dots\})|_{g^N}}{\int_0^1 \frac{d\alpha}{\alpha} W_1(\{\alpha, 1, \dots; 1, 1, \dots\})|_{g^N}} \quad (3.10)$$

3.3. General solution for finite distances

From now on, we will concentrate on the study of the *local* environment of a given vertex. By this, we mean the statistics of edges and vertices within a *finite* range, say k , of geodesic distances from an origin. To this end, we may limit ourselves to a finite set of parameters $\{\alpha_1, \dots, \alpha_k; \rho_1, \dots, \rho_k\}$ while all other α 's and ρ 's are taken equal to one. Here

we wish to present a very general scheme for solving this problem in the form of algebraic equations for the generating functions.

Introducing the functions

$$Z_j = \alpha_j W_j \quad (3.11)$$

the equations (3.7) split into two sets of equations: a finite set

$$\begin{aligned} Z_j &= \frac{\alpha_j \rho_j}{1 - g\alpha_j(Z_{j+1} + Z_j + Z_{j-1})} \quad (\text{Q.}) \\ Z_j &= \frac{\alpha_j \rho_j}{1 - g\alpha_j(Z_{j+1} + Z_{j-1})} \quad (\text{E.T.}) \end{aligned} \quad (3.12)$$

valid for $1 \leq j \leq k$, and an infinite set

$$\begin{aligned} Z_j &= \frac{1}{1 - g(Z_{j+1} + Z_j + Z_{j-1})} \quad (\text{Q.}) \\ Z_j &= \frac{1}{1 - g(Z_{j+1} + Z_{j-1})} \quad (\text{E.T.}) \end{aligned} \quad (3.13)$$

for all $j \geq k+1$. Remarkably enough, this latter infinite set of equations may be replaced by a *single equation*. Indeed, these equations may be solved order by order in g from the initial data Z_k . Moreover, it is clear from the interpretation of the $Z_j = W_j$ for $j \geq k+1$ that $Z_j \rightarrow W$ as in (3.3) when $j \rightarrow \infty$. This is equivalently ensured by a single relation between Z_{k+1} and Z_k thanks to the existence of a *discrete integral of motion* $f(Z_j, Z_{j+1}) = f(Z_{j+1}, Z_{j+2})$ $j \geq k$, with

$$\begin{aligned} f(x, y) &= xy(1 - g(x + y)) - x - y \quad (\text{Q.}) \\ f(x, y) &= xy(1 - gx)(1 - gy) + gxy - x - y \quad (\text{E.T.}) \end{aligned} \quad (3.14)$$

The convergence is ensured by writing

$$f(Z_k, Z_{k+1}) = f(W, W) \quad (3.15)$$

This equation is now supplemented by the finite set (3.12) of k equations, and upon elimination we may write a single algebraic equation for say $W_1 = Z_1/\alpha_1$.

As an illustration, let us work out the case $k = 0$ where all α 's and ρ 's are one. We get a single equation $f(0, W_1) = -W_1 = f(W, W)$, which yields

$$\begin{aligned} W_1 &= W - gW^3 \quad (\text{Q.}) \\ W_1 &= 1 + gW^3(1 - 3gW) \quad (\text{E.T.}) \end{aligned} \quad (3.16)$$

in agreement with the results (3.5).

The case $k = 1$ of the statistics of nearest neighboring edges and vertices will be studied extensively in the next section.

For fixed k , we have also access to the statistics of finitely distant edges and vertices from a vertex in *infinite* graphs, defined as the limit $N \rightarrow \infty$ of the statistics at fixed N . In particular, we may define

$$\Gamma(\{\alpha_1, \dots, \alpha_k; \rho_1, \dots, \rho_k\}) = \lim_{N \rightarrow \infty} \Gamma_N(\{\alpha_1, \dots, \alpha_k, 1, \dots; \rho_1, \dots, \rho_k, 1, \dots\}) \quad (3.17)$$

Eq.(3.10) translates into

$$\Gamma(\{\alpha_1, \dots, \alpha_k; \rho_1, \dots, \rho_k\}) = \frac{\int_0^{\alpha_1} \frac{d\alpha}{\alpha} W_1(\{\alpha, \alpha_2, \dots, \alpha_k, 1, \dots; \rho_1, \rho_2, \dots, \rho_k, 1, \dots\})|_{\text{sing}}}{\int_0^1 \frac{d\alpha}{\alpha} W_1(\{\alpha, 1, \dots; 1, 1, \dots\})|_{\text{sing}}} \quad (3.18)$$

where the subscript $|_{\text{sing}}$ refers to the singular part of the corresponding function of g as g approaches the critical value $g_c = 1/12$ (Q.) or $g_c = 1/8$ (E.T.), proportional to $(g_c - g)^{3/2}$ both in the numerator and denominator of eq.(3.18), as we shall see in next section.

4. Nearest neighbor statistics: general solution

In this section as well as in the next two ones, we address the question of *nearest* neighbor statistics, for which explicit and particularly simple formulas may be written. Here we concentrate first on the case of quadrangulations and then repeat our analysis for Eulerian triangulations.

4.1. Quadrangulations

Combining the equations (3.12) and (3.15) for $k = 1$ in the case of quadrangulations, we obtain the following third degree algebraic equation, with $\alpha \equiv \alpha_1$ and $\rho \equiv \rho_1$

$$(W_1 - \rho)(W_1(\alpha - 1) + \rho - 1) - g\alpha W_1(W_1^2\alpha(\alpha - 1) + \alpha\rho W_1 + W(W - 2)) + 2g^2\alpha W^3 W_1 = 0 \quad (4.1)$$

We must pick the unique solution of eq.(4.1) with a g series expansion, and such that $W_1 = \rho + O(g)$. We get

$$W_1 = \rho + g\alpha\rho(1 + \alpha\rho) + g^2\alpha\rho(2 + \alpha + \alpha\rho + 3\alpha^2\rho + 2\alpha^3\rho^2) + O(g^3) \quad (4.2)$$

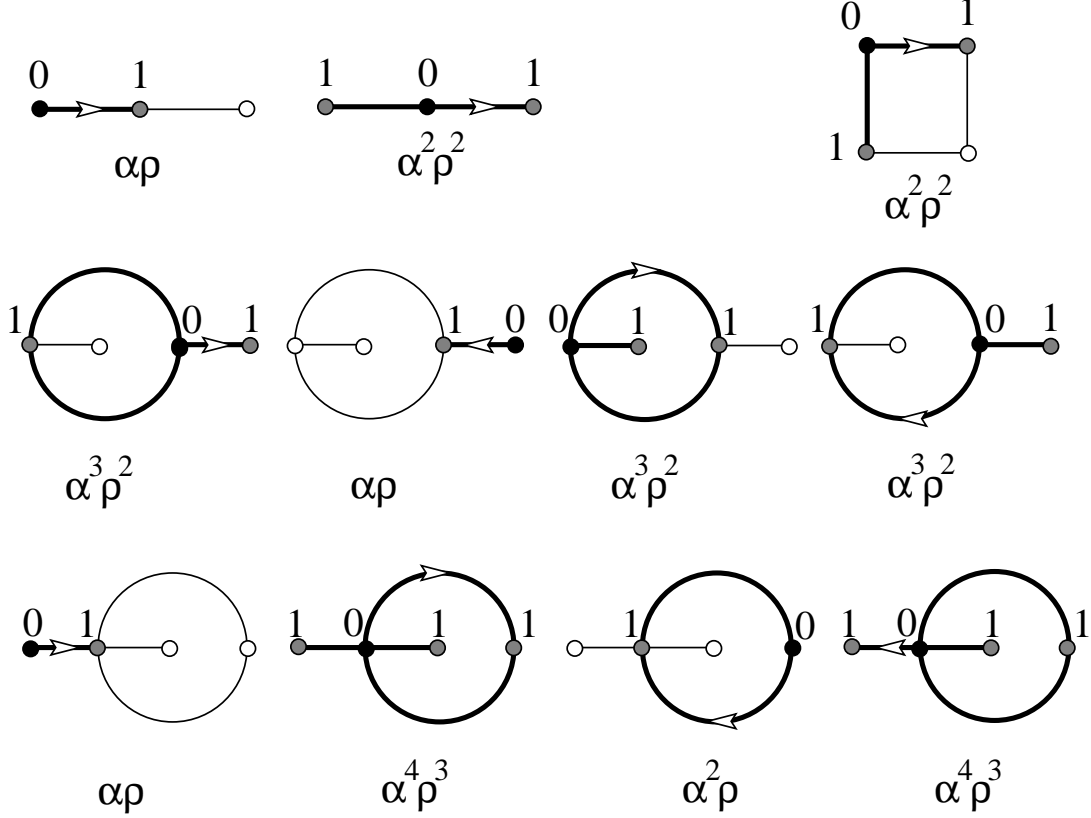


Fig.12: The rooted planar quadrangulations with up to two faces, and the corresponding weights α per nearest neighboring edge (represented in thick solid line) of the origin (labeled 0), and ρ per nearest neighboring vertex (represented in grey, and labeled 1). These weights match the expansion (4.2) of W_1 .

up to order 2 in g , in agreement with the direct enumeration of the quadrangulations with up to two faces (see Fig.12).

We may now study in detail the statistics of nearest neighbors in *infinite* quadrangulations by letting $g \rightarrow g_c = 1/12$. Close to this critical point we write

$$g = \frac{1}{12}(1 - \epsilon^2), \quad W = \frac{2}{1 + \epsilon} \quad (4.3)$$

and substitute the expanded solution $W_1 = a + b\epsilon + c\epsilon^2 + d\epsilon^3 + O(\epsilon^4)$ into the cubic equation (4.1). At order 0 in ϵ , we find that

$$F(a|\alpha; \rho) \equiv 36\rho(\rho-1) + 4a(9-\alpha-18\rho+9\alpha\rho) + 3a^2(12(1-\alpha)+\alpha^2\rho) + 3a^3\alpha^2(\alpha-1) = 0 \quad (4.4)$$

which fixes a as the unique solution with value $4/3$ at $\alpha = \rho = 1$, extracted from the solution (3.5) at $\theta = \sqrt{\epsilon} = 0$. Alternatively, this solution also satisfies $a = \rho + O(\alpha)$ as a

series of α , and this latter property also fixes it entirely among the three possible solutions of $F(a) = 0$. Moreover we find at order one in ϵ that $b = 0$, and the most singular ($\propto (g_c - g)^{3/2}$) term d , obtained at order 3 in ϵ , is related to a via

$$W_1(\alpha; \rho)|_{\text{sing}} = d = \frac{8\alpha a}{\partial_a F(a|\alpha; \rho)} \quad (4.5)$$

with F as in eq.(4.4). Finally, let us perform the change of variable $\alpha \rightarrow A = \alpha a$ in the integrals of eq.(3.18). Using the explicit expression of α in terms of A :

$$\alpha = \frac{3}{2}A \frac{12A + A^2 + 24\rho - 12 - (2 - A)\sqrt{(18 - A)(2 - A)}}{36\rho(\rho + A - 1) + A(3A\rho + 3A^2 - 4)} \quad (4.6)$$

as well as $d\alpha/dA = -\partial_a F / ((A/\alpha)\partial_a F - \alpha\partial_\alpha F)$, we get

$$\Gamma \equiv \Gamma(\alpha; \rho) = \frac{\int_0^A dy \frac{8(y/\alpha)}{(y/\alpha)\partial_a F(y/\alpha|\alpha, \rho) - \alpha\partial_\alpha F(y/\alpha|\alpha; \rho)}}{\int_0^{4/3} dy \frac{8y}{(y\partial_a F(y|1; 1) - \partial_\alpha F(y|1; 1))}} = \frac{1}{2} \left(\sqrt{\frac{18 - A}{2 - A}} - 3 \right) \quad (4.7)$$

This remarkably simple formula is easily inverted into

$$A = 2 \frac{\Gamma(\Gamma + 3)}{(\Gamma + 1)(\Gamma + 2)} \quad (4.8)$$

itself mysteriously reminiscent of the form of the solution (3.2). To determine Γ , we finally note that $a = A/\alpha$ being a root of the cubic equation (4.4), we may write a cubic equation for Γ as well:

$$6\Gamma(1 + \Gamma)(3 + \Gamma) - \alpha(2\Gamma(1 + 4\Gamma + \Gamma^2) + 3\rho(1 + \Gamma)^2(2 + \Gamma)) = 0 \quad (4.9)$$

which fixes Γ uniquely by the condition that $\Gamma = 1$ for $\alpha = \rho = 1$, or alternatively by $\Gamma = 0$ when $\alpha = 0$.

4.2. Eulerian triangulations

Combining the equations (3.12) and (3.15) for $k = 1$ in the case of Eulerian triangulations, and taking again $\alpha_1 \equiv \alpha$, $\rho_1 \equiv \rho$, we get the following algebraic equation of degree three for $W_1 = Z_1/\alpha$:

$$\begin{aligned} &(\rho - W_1)(W_1(\alpha - 1) + \rho - 1) + g\alpha W_1(W(W - 2) + (\alpha - 1)W_1(W_1 + 1) \\ &+ \rho(1 + 2W_1 - W_1\alpha - \rho)) + g^2\alpha W_1 W^2(1 - 2W) + g^3\alpha W^4 W_1 = 0 \end{aligned} \quad (4.10)$$

Again, we must pick the unique solution of eq.(4.10) with a g series expansion, such that $W_1 = \rho + O(g)$, whose first terms read

$$W_1 = \rho + g\alpha\rho + g^2\alpha\rho(1 + \alpha + \alpha\rho) + g^3\alpha\rho(3 + 2\alpha + \alpha^2 + 2\alpha\rho + 3\alpha^2\rho + \alpha^2\rho^2) + O(g^4) \quad (4.11)$$

up to order 3 in g , in agreement with the graphs of Fig.13.

Close to the critical point we write

$$g = \frac{1}{8}(1 - \epsilon^2), \quad W = \frac{2}{1 + \epsilon} \quad (4.12)$$

and substitute the expanded solution $W_1 = a + b\epsilon + c\epsilon^2 + d\epsilon^3 + O(\epsilon^4)$ into the cubic equation (4.10). At order 0 in ϵ , we find that

$$\begin{aligned} F(a|\alpha; \rho) &\equiv 32\rho(\rho - 1) + a(32 - 5\alpha - 64\rho + 4\alpha\rho(9 - \rho)) \\ &+ 4a^2((\alpha - 1)(\alpha - 8) - \alpha\rho(\alpha - 2)) + 4a^3\alpha(\alpha - 1) = 0 \end{aligned} \quad (4.13)$$

which fixes a as the unique solution with value $5/4$ at $\alpha = \rho = 1$, extracted from the solution (3.5) at $\theta = \sqrt{\epsilon} = 0$. As before, this solution also satisfies $a = \rho + O(\alpha)$, which fixes it entirely among the three possible solutions of $F(a) = 0$. Again, we find at order one in ϵ that $b = 0$, and the most singular ($\propto (g_c - g)^{3/2}$) term d is obtained at order 3 in ϵ . It is related to a via

$$W_1(\alpha; \rho)|_{\text{sing}} = d = \frac{8\alpha a}{\partial_a F(a|\alpha; \rho)} \quad (4.14)$$

with F as in eq.(4.13). Finally, let us perform the change of variable $\alpha \rightarrow A = \alpha a$ in the integrals of eq.(3.18). Using the explicit expression of α in terms of A :

$$\alpha = 2A \frac{9A - A^2 + 16\rho - 2A\rho - 8 - (2 - A)\sqrt{(8 - A)(2 - A)}}{32\rho(\rho - 1) + 36A\rho - 4A^2\rho - 4A\rho^2 + 4A^2 - 5A} \quad (4.15)$$

as well as $d\alpha/dA = -\partial_a F / ((A/\alpha)\partial_a F - \alpha\partial_\alpha F)$, we get

$$\Gamma \equiv \Gamma(\alpha; \rho) = \frac{\int_0^A dy \frac{8(y/\alpha)}{(y/\alpha)\partial_a F(y/\alpha|\alpha, \rho) - \alpha\partial_\alpha F(y/\alpha|\alpha; \rho)}}{\int_0^{5/4} dy \frac{8y}{(y\partial_a F(y|1; 1) - \partial_\alpha F(y|1; 1))}} = \sqrt{\frac{8 - A}{2 - A}} - 2 \quad (4.16)$$

easily inverted into

$$A = 2 \frac{\Gamma(\Gamma + 4)}{(\Gamma + 1)(\Gamma + 3)} \quad (4.17)$$

also reminiscent of the form of the solution (3.2). We may again use eq.(4.13) to write a cubic equation for Γ :

$$4\Gamma(\Gamma + 2)(\Gamma + 4) - \alpha(\Gamma + 1)(\Gamma(\Gamma + 5) + 2\rho(\Gamma + 2)(\Gamma + 3)) = 0 \quad (4.18)$$

and Γ is fixed uniquely by the condition that $\Gamma = 1$ for $\alpha = \rho = 1$, or alternatively by $\Gamma = 0$ when $\alpha = 0$.

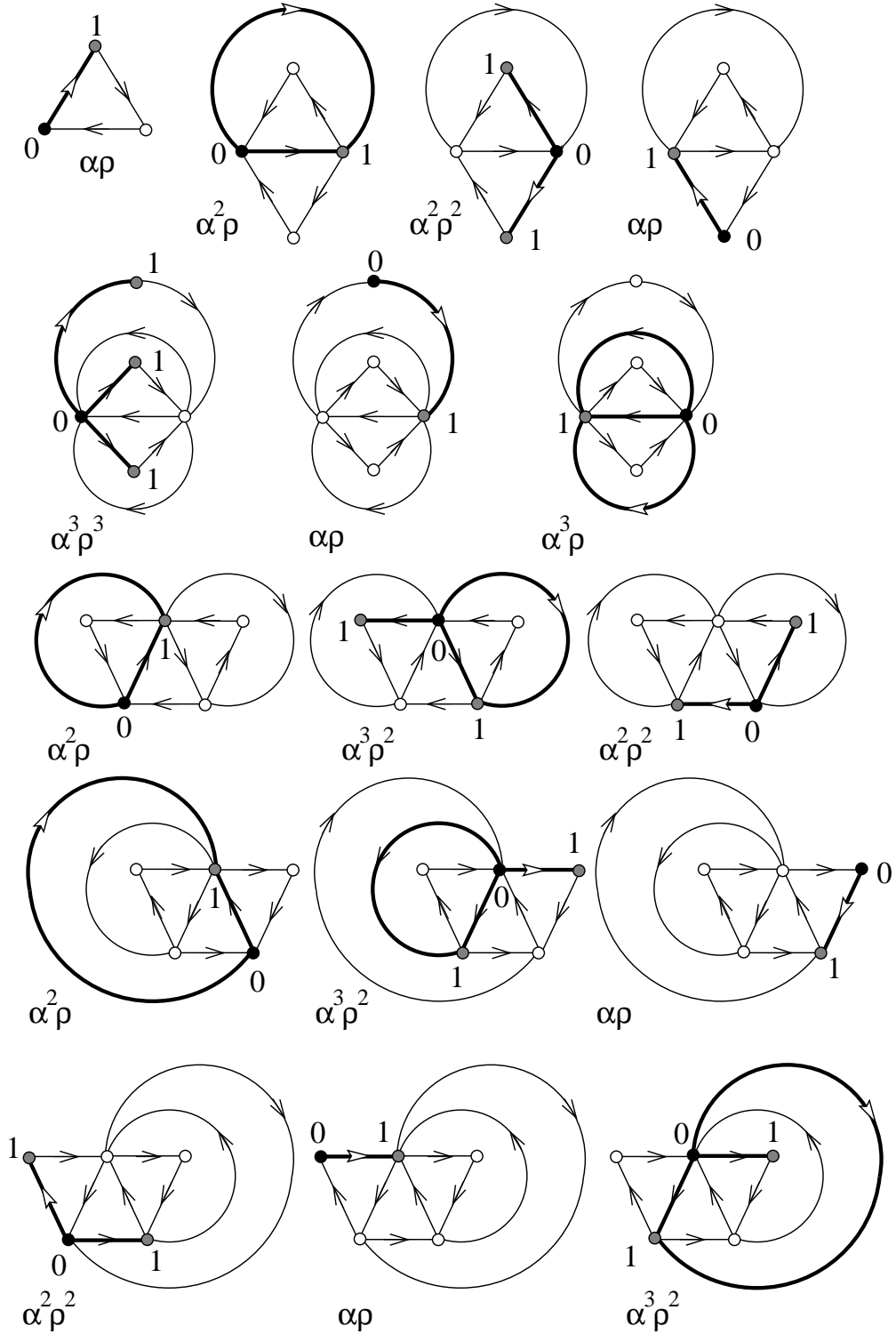


Fig.13: The rooted planar Eulerian triangulations with up to 6 faces, and the corresponding weights α per nearest neighboring edge (represented in thick solid line) from the origin (labeled 0), and ρ per nearest neighboring vertex (represented in grey, and labeled 1). These weights match the expansion (4.11) of W_1 .

5. Nearest neighbor statistics: probabilities and moments

5.1. Quadrangulations

We may extract from the solution of eq.(4.9) various probabilities and moments for the numbers of nearest neighboring edges or vertices of a given vertex in infinite quadrangulations. Taking for instance $\alpha = 1$, the solution reads

$$\Gamma(1; \rho) = \frac{2}{\sqrt{4-3\rho}} - 1 = \sum_{n \geq 1} \rho^n \left(\frac{3}{16}\right)^n \binom{2n}{n} \quad (5.1)$$

in which we read the probability

$$P(n) = \left(\frac{3}{16}\right)^n \binom{2n}{n} \quad (5.2)$$

that a vertex have n nearest neighboring vertices. Analogously, taking $\rho = 1$, we get

$$\Gamma(\alpha; 1) = \frac{1}{2} \left(\sqrt{\frac{3(2+\alpha)}{6-5\alpha}} - 1 \right) = \frac{1}{3}\alpha + \frac{1}{6}\alpha^2 + \frac{13}{108}\alpha^3 + \dots \quad (5.3)$$

in which we read the probabilities $1/3, 1/6, 13/108, \dots$ for having $1, 2, 3, \dots$ nearest neighboring edges.

The formulae (5.1) and (5.3) also yield the various moments of the distribution of the numbers n_1 and m_1 of nearest neighboring vertices and edges, upon writing $\rho = e^u$ (resp. $\alpha = e^v$) and expanding around $u = 0$ (resp. $v = 0$). For instance we get

$$\begin{aligned} \langle n_1 \rangle &= 3, & \langle n_1^2 \rangle &= \frac{33}{2}, & \langle n_1^3 \rangle &= \frac{579}{4} \\ \langle m_1 \rangle &= 4, & \langle m_1^2 \rangle &= \frac{100}{3}, & \langle m_1^3 \rangle &= \frac{1372}{3} \end{aligned} \quad (5.4)$$

The value $\langle m_1 \rangle = 4$ does not come as a surprise, as for each quadrangulation \mathcal{G} with N faces, we have $\sum_{v \in \mathcal{G}} m_1(\mathcal{G}, v) = 4N$ (twice the total number of edges), while there are $N + 2$ vertices, hence $\langle m_1 \rangle_N = 4N/(N + 2) \rightarrow 4$ for large N .

More generally, we have access to the joint probabilities for the numbers of nearest neighboring edges and vertices and to the associated mixed moments by expanding Γ as a double power series of α and ρ around 0 (probabilities) or 1 (moments).

Finally, we also have access to the conditional probabilities of having n nearest neighboring vertices *given that there are no multiple nearest neighbors*. This is achieved by taking $\rho = t/\alpha$, in which case $\Gamma = \langle \alpha^{m_1 - n_1} t^{n_1} \rangle$, and then sending $\alpha \rightarrow 0$ to retain only

the configurations where $m_1 = n_1$ (as $m_1 \geq n_1$ always). This results in the generating function $\Pi(t)/\Pi(1)$ for the above conditional probabilities, where

$$\Pi(t) \equiv \lim_{\alpha \rightarrow 0} \Gamma(\alpha; \frac{t}{\alpha}) = \frac{1}{2} \left(\sqrt{\frac{18-t}{2-t}} - 3 \right) = \frac{1}{3}t + \frac{7}{54}t^2 + \frac{53}{972}t^3 + \dots \quad (5.5)$$

and in particular we get the probability of having no multiple nearest neighbor $\Pi(1) = (\sqrt{17}-3)/2$. We note that from eq.(4.7) we have $\Pi(A) = \Gamma$. This relation is not surprising, once understood in the language of well-labeled trees. Indeed, the trees contributing to $\Pi(t)$ are those associated with graphs without multiple nearest neighbors of the origin, i.e. those in which the vertices labeled 1 are all terminal (univalent) vertices and receive a weight t . Replacing this weight t by $Z_1 = \alpha W_1$ reconstructs the full generating function contributing to Γ . For large graphs, this corresponds to the substitution $t \rightarrow A$ in Π .

5.2. Eulerian triangulations

Repeating the various specializations of previous section of the solution to eq.(4.18), we get for $\alpha = 1$:

$$\Gamma(1; \rho) = \frac{1}{2} \left(\sqrt{\frac{27-2\rho}{3-2\rho}} - 3 \right) = \frac{4}{9}\rho + \frac{56}{243}\rho^2 + \frac{848}{6561}\rho^3 + \dots \quad (5.6)$$

leading to the probabilities $4/9, 56/243, 848/6561, \dots$ that a vertex have 1, 2, 3, \dots nearest neighboring vertices. For $\rho = 1$, we get:

$$\Gamma(\alpha; 1) = \frac{2}{\sqrt{4-3\alpha}} - 1 \quad (5.7)$$

in which we read the probability

$$P(m) = \left(\frac{3}{16} \right)^m \binom{2m}{m} \quad (5.8)$$

for having m nearest neighboring edges. Remarkably, these probabilities for nearest neighboring *edges* in Eulerian triangulations coincide with those of eq.(5.2) for nearest neighboring *vertices* in quadrangulations. Note also that the probability (5.8) is very similar to that obtained in Ref.[8] for ordinary triangulations with no multiple edge and no loop.

The corresponding moments read

$$\begin{aligned} \langle n_1 \rangle &= \frac{12}{5}, & \langle n_1^2 \rangle &= \frac{1212}{125}, & \langle n_1^3 \rangle &= \frac{190236}{3125} \\ \langle m_1 \rangle &= 3, & \langle m_1^2 \rangle &= \frac{33}{2}, & \langle m_1^3 \rangle &= \frac{579}{4} \end{aligned} \quad (5.9)$$

The value $\langle m_1 \rangle = 3$ can be obtained by explicitly computing $\langle m_1 \rangle_N = 3N/(N+2) \rightarrow 3$ for large N .

Finally, we also have the conditional probabilities of having n nearest neighboring vertices given that there are no multiple nearest neighbors. Repeating the limiting process of previous section we arrive at

$$\Pi(t) \equiv \lim_{\alpha \rightarrow 0} \Gamma(\alpha; \frac{t}{\alpha}) = \sqrt{\frac{8-t}{2-t}} - 2 = \frac{3}{8}t + \frac{39}{256}t^2 + \frac{267}{4096}t^3 + \dots \quad (5.10)$$

and in particular we get the probability of having no multiple nearest neighbor $\Pi(1) = \sqrt{7} - 2$. As before, we have $\Pi(A) = \Gamma$ of eq.(4.16).

6. Heuristic interpretation: Phase diagram

The results of previous section display a number of critical values of α and ρ at which the various generating functions become singular. For quadrangulations we have singular points at $(\alpha = 1; \rho = 4/3)$ and $(\alpha = 6/5; \rho = 1)$, easily read off eqs.(5.1) and (5.3). The value $\rho^{-1} = 3/4$ (resp. $\alpha^{-1} = 5/6$) governs the exponential decay of the corresponding probabilities, behaving as $(3/4)^n$ (resp. as $(5/6)^m$). Similarly, for Eulerian triangulations, we have the particular points $(\alpha = 1; \rho = 3/2)$ and $(\alpha = 4/3; \rho = 1)$, read off eqs.(5.6) and (5.7). These points are particular points on a more general critical curve in the (α, ρ) plane, whose location may be easily obtained from the following heuristic argument.

Labeled trees may be thought of as trees embedded in a one-dimensional target space, by viewing the labels as the positions of the vertices in the target space. In this language, the generating function W_j corresponds to trees with a root at *position* j . Without the constraint that the labels remain positive, all W_j 's are equal to W of eq.(3.3), with $W|_{g^N} = 3^N c_N$ (Q.) or $2^N c_N$ (E.T.), counting arbitrary rooted planar trees with N edges (in number c_N) together with 3^N (resp. 2^N) embeddings accounting for the 3 (resp. 2) possibilities of labeling a vertex according to the label of its immediate ascendent vertex.

The positivity of all labels simply restricts the target space to a half-line, by introducing a hard wall at the origin, whose effect is to reduce the entropy when compared with the no-wall situation. On the other hand, the weights α and ρ of Sect.4 act as energy weights when an edge or a vertex touches the wall, which may help restore the balance between the reduction of entropy and a possible gain in energy. The critical curve corresponds to an unbinding transition at which the balance is realized. Its location may be obtained

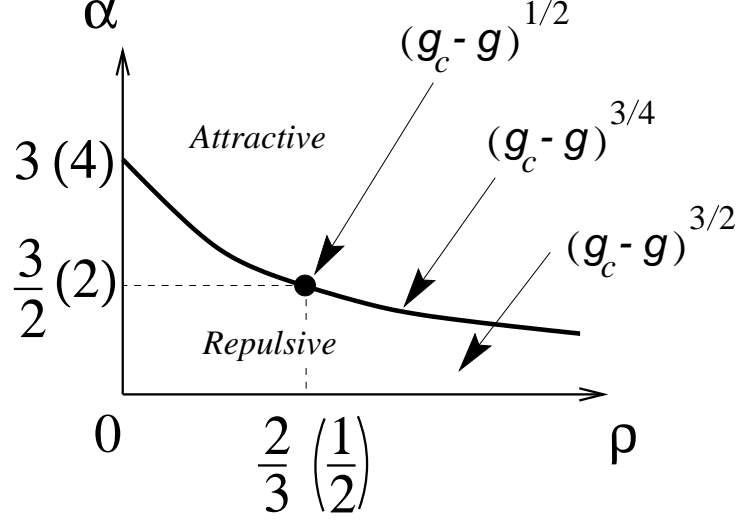


Fig.14: Phase diagram in the (ρ, α) plane for rooted trees embedded in a one-dimensional target space with a wall and weights α (resp. ρ) per edge (resp. vertex) touching the wall. A critical curve separates a region where the tree is attracted by the wall from a region where it is repulsed by it. This curve possesses a higher order (tricritical) point represented by a black dot. The corresponding leading singular behavior of W_1 is indicated. The indicated values of α and ρ refer to well-labeled trees associated to quadrangulations (Eulerian triangulations).

as follows. For each vertex of the tree reaching position 1, we have an energy gain $\rho\alpha^k$, where k is the number of nearest neighbors of the vertex on the tree. On the other hand, the entropy loss is $(2/3)^{k-1}$ (Q.) or $1/2^{k-1}$ (E.T.) as the $k-1$ descendents of this vertex have lost one of their 3 (resp. 2) possible positions. In an infinite rooted planar tree, the probability of having k neighbors is $1/2^k$, hence the balance is reached when

$$\begin{aligned}
 1 &= \sum_{k \geq 1} \frac{1}{2^k} \rho \alpha^k \left(\frac{2}{3}\right)^{k-1} = \frac{3}{2} \frac{\rho \alpha}{3 - \alpha} \quad (\text{Q.}) \\
 1 &= \sum_{k \geq 1} \frac{1}{2^k} \rho \alpha^k \frac{1}{2^{k-1}} = \frac{2\rho\alpha}{4 - \alpha} \quad (\text{E.T.})
 \end{aligned} \tag{6.1}$$

This displays the critical lines $2(3 - \alpha) = 3\rho\alpha$ (Q.) or $4 - \alpha = 2\rho\alpha$ (E.T.) separating a phase in which the tree is “attracted” by the wall from a phase where it is “repulsed” by it (see Fig.14). All pairs $(\alpha; \rho)$ mentioned above belong to these critical lines. A special point on these lines corresponds to the *exact balance* for *each* separate value of the valence k , namely when $\rho\alpha^k = (3/2)^{k-1}$ (Q.) or $\rho\alpha^k = 2^{k-1}$ (E.T.) for all $k \geq 1$, i.e. $\alpha = 3/2, \rho = 2/3$ or $\alpha = 2, \rho = 1/2$ (E.T.). At this special point, the effect of the wall is exactly suppressed and the half-line solution coincides with the no-wall solution, namely $Z_j = W$ for all $j \geq 1$.

Therefore at this special point, the singularity of $W_1 = \rho W$ is proportional to $(g_c - g)^{1/2}$, instead of the generic singularity $\propto (g_c - g)^{3/2}$ already observed away from the critical line. It is easily checked that the generic singularity along the critical line is of the form $(g_c - g)^{3/4}$, easily obtained by expanding the equations (4.1) and (4.10) now in powers of $\theta = \sqrt{\epsilon}$ and solving order by order for the coefficients of $W_1 = A + B\theta + C\theta^2 + D\theta^3 + \dots$. These various critical behaviors translate into different asymptotics for the weighted sums over graphs of size N , of the form g_c^{-N}/N^γ with $\gamma = 5/2$ (most generic case, away from the critical line), $\gamma = 7/4$ (generic on the critical line) and $\gamma = 3/2$ (special point on the critical line).

Beside the above heuristic argument, the critical lines may also be derived by imposing that both $F(a|\alpha; \rho) = 0$ and $\partial_a F(a|\alpha; \rho) = 0$ (with F as in eqs.(4.4) or (4.13)), while the special (tricritical) point corresponds to having in addition $\partial_a^2 F(a|\alpha; \rho) = 0$.

7. Generalization to more distant neighbors

7.1. General scheme for getting Γ

The results of Sects. 4 and 5 may be generalized so as to include more distant neighbors, say up to k -th neighboring edges and vertices. This involves explicitly solving the equations (3.12) and (3.15). The resulting algebraic equation for W_1 however grows in degree with k , and one still has to integrate once with respect to α_1 to finally obtain the statistical average Γ of eq.(3.18). Nevertheless, we have found a particularly simple alternative way of getting Γ by relating it to a single quantity t parametrizing all Z_j 's *at the critical point*. More precisely, when $g = g_c$, with $g_c = 1/12$ (Q.) or $g_c = 1/8$ (E.T.) and $W = W_c = 2$, $x = x_c = 1$ (as readily seen from eqs.(3.3) and (3.4)), the convergence condition (3.15) is trivialized by a change of variables on $Z_k = Z_k^c$ borrowed from the exact solution. Namely, if we write

$$Z_j^c \equiv \zeta_j(t_j), \quad \text{with} \quad \begin{cases} \zeta_j(t) = 2 \frac{(t+j)(t+j+3)}{(t+j+1)(t+j+2)} & \text{(Q.)} \\ \zeta_j(t) = 2 \frac{(t+j)(t+j+4)}{(t+j+1)(t+j+3)} & \text{(E.T.)} \end{cases} \quad (7.1)$$

for all $j \geq k$, then the condition $f(Z_j^c, Z_{j+1}^c) = f(2, 2)$ amounts to $t_j = t_{j+1}$, hence $t_j = t$ for all $j \geq k$. The value of t is obtained via the set of k equations (3.12), which we feed with the two “final conditions” $Z_k^c = \zeta_k(t)$ and $Z_{k+1}^c = \zeta_{k+1}(t)$, allowing to express backward all Z_j^c 's with $j < k$ as rational functions of t and to finally get one algebraic equation for t with α 's and ρ 's as parameters. The proper solution is then uniquely characterized by the

fact that when all α 's and ρ 's are one, we have $t = 0$, as can be read off the solution (3.2) at criticality, where $W = 2$ and $u_j \propto j$.

Quite magically, it turns out that t may be identified with the desired function Γ , up to a translation independent of α_1 . More precisely, we have

$$\Gamma(\{\alpha_i; \rho_i\}) = t(\{\alpha_1, \alpha_2, \dots; \rho_1, \rho_2, \dots\}) - t(\{0, \alpha_2, \dots; \rho_1, \rho_2, \dots\}) \quad (7.2)$$

as Γ must vanish when $\alpha_1 = 0$ (note that when $\alpha_1 = 0$, $Z_1 = 0$ and t does not depend on ρ_1 either). This remarkable identity may be checked at $k = 1$ where $t(\{0, 1, 1, \dots; \rho_1, 1, 1, \dots\}) = t(\{0, 1, 1, \dots; 0, 1, 1, \dots\}) = -1$ (the solution is the same as when all α 's and ρ 's are one except for a shift in the indices) and the relation $\Gamma = t + 1$ is read off eqs. (4.8) and (4.17) with $A = Z_1^c$. For arbitrary k , the identification (7.2) will be proved in the next section thanks to scaling arguments.

The value of Γ may therefore be extracted as follows: let $G(t) \equiv G(t|\{\alpha_i; \rho_i\}) = 0$ denote the algebraic equation satisfied by t . Then if we take $\alpha_1 = 0$ we get an algebraic equation $G_0(t_0) = 0$ for the translation parameter $t_0 \equiv t(\{0, \alpha_2, \dots; \rho_1, \rho_2, \dots\})$ of eq.(7.2). We therefore simply have to eliminate t_0 between the two equations $G(\Gamma + t_0) = 0$ and $G_0(t_0) = 0$ to get an equation for Γ . This equation might be sometimes factorized into smaller degree equations, but the initial condition $\Gamma = O(\alpha_1)$ always selects only one of them. For illustration, we will recover in Sect. 7.3 below the results for Γ at $k = 1$, and further present the solution for $k = 2$.

7.2. The reason why $t = \Gamma + t_0$

In this section we show that the parameter t occurring in the changes of variables

$$\begin{aligned} Z_j^c &= 2 \frac{(t+j)(t+j+3)}{(t+j+1)(t+j+2)} & (\text{Q.}) \\ Z_j^c &= 2 \frac{(t+j)(t+j+4)}{(t+j+1)(t+j+3)} & (\text{E.T.}) \end{aligned} \quad (7.3)$$

coincides with the statistical average Γ up to an additive constant independent of α_1 . We simply have to show that $dt/d\alpha_1 = d\Gamma/d\alpha_1$. Let us first find a simpler characterization of t , by considering Z_j^c at large j . Expanding Z_j^c at large $j \geq k$, we find

$$\begin{aligned} Z_j^c &= 2 - \frac{4}{j^2} + \frac{8}{j^3}(t + \frac{3}{2}) + O(\frac{1}{j^4}) & (\text{Q.}) \\ Z_j^c &= 2 - \frac{6}{j^2} + \frac{12}{j^3}(t + 2) + O(\frac{1}{j^4}) & (\text{E.T.}) \end{aligned} \quad (7.4)$$

therefore t enters only the subleading correction $\propto 1/j^3$ of Z_j^c . Let us now go back to the combinatorial interpretation of Z_j (for large enough j) as a series of g , before taking $g \rightarrow g_c$. We see that $dZ_j/d\alpha_1$ is the generating function for well-labeled trees with a root at position j and a *marked oriented edge* originating from a vertex at position 1. In terms of graphs⁵, consider the generating function $G_j(\{\alpha_i; \rho_i\})$ for graphs with a marked vertex (origin) and a marked edge from a vertex at geodesic distance $j - 1$ from the origin to a vertex at geodesic distance j from the origin. Then we have

$$\begin{aligned} G_j(\{\alpha_1, \alpha_2, \dots, \alpha_k; \rho_1, \rho_2, \dots, \rho_k\}) \\ = Z_j(\{\alpha_1, \alpha_2, \dots, \alpha_k; \rho_1, \rho_2, \dots, \rho_k\}) - Z_{j-1}(\{\alpha_2, \alpha_3, \dots, \alpha_k; \rho_2, \rho_3, \dots, \rho_k\}) \end{aligned} \quad (7.5)$$

Indeed, in the tree language, G_j generates the well-labeled trees with root at position j and which *do reach* the position 1, therefore expressed via (7.5) by subtracting from the generating function $Z_j(\{\alpha_i; \rho_i\})$ the contribution of trees which do not reach position 1, also equal to that of trees with root at position $j - 1$, provided we shift the whole picture by -1 , thus removing the terms α_1, ρ_1 pertaining to position 1. Taking a derivative of eq.(7.5) with respect to α_1 , we see that $dZ_j/d\alpha_1 = dG_j/d\alpha_1$. With this identification, we have

$$\frac{\alpha_1 \frac{dZ_j}{d\alpha_1} |_{g^N}}{W_1(\{1; 1\})|_{g^N}} = \frac{\langle m_1 m_j \prod \alpha_i^{m_i} \rho_i^{n_i} \rangle_N}{\langle m_1 \rangle_N} \quad (7.6)$$

When $N \rightarrow \infty$, we deduce that

$$\frac{\alpha_1 \frac{dZ_j}{d\alpha_1} |_{\text{sing}}}{W_1(\{1; 1\})|_{\text{sing}}} = \frac{\langle m_1 m_j \prod \alpha_i^{m_i} \rho_i^{n_i} \rangle}{\langle m_1 \rangle} \quad (7.7)$$

where $\langle \dots \rangle$ with no index N refers to the large N limit. For large j we expect the average in the numerator to factor into $\langle m_j \rangle \langle m_1 \prod \alpha_i^{m_i} \rho_i^{n_i} \rangle$ as the weights are localized around the origin (k is kept finite). We arrive at the relation

$$\lim_{j \rightarrow \infty} \frac{\frac{dZ_j}{d\alpha_1} |_{\text{sing}}}{\langle m_j \rangle} = \frac{W_1(\{1; 1\})|_{\text{sing}}}{\langle m_1 \rangle} \frac{d\Gamma}{d\alpha_1} = \frac{2}{3} \frac{d\Gamma}{d\alpha_1} \quad (7.8)$$

for both quadrangulations and Eulerian triangulations: indeed we have used $\langle m_1 \rangle = 4$ and $W_1(\{1; 1\})|_{\text{sing}} = 8/3$ (Q.) while $\langle m_1 \rangle = 3$ and $W_1(\{1; 1\})|_{\text{sing}} = 2$ (E.T.) from eqs.(4.5) and (4.14) at $\alpha = \rho = 1$.

⁵ Here and throughout the appendix, the mention graph refers to either quadrangulations or Eulerian triangulations.

Both $\langle m_j \rangle$ and $dZ_j/d\alpha_1|_{\text{sing}}$ may be computed by considering the usual scaling limit reached by sending *simultaneously* $g \rightarrow g_c$ and $j \rightarrow \infty$, say by setting

$$g = g_c(1 - \theta^2), \quad j = \frac{r}{\theta} \quad (7.9)$$

and letting $\theta \rightarrow 0$ (here θ^{-1} plays the role of a correlation length for the models at hand). In this limit, we have

$$Z_j = 2(1 - \theta^2 \mathcal{U}(r) - \theta^3 \mathcal{V}(r) - \dots) \quad (7.10)$$

Upon substituting this expression for Z_j into eqs.(3.13), we obtain at order 4 and 5 in θ the following differential equations

$$\begin{aligned} \mathcal{U}'' &= 3(\mathcal{U}^2 - 1) & \mathcal{V}'' &= 6\mathcal{U}\mathcal{V} & (\text{Q.}) \\ \mathcal{U}'' &= 2(\mathcal{U}^2 - 1) & \mathcal{V}'' &= 4\mathcal{U}\mathcal{V} & (\text{E.T.}) \end{aligned} \quad (7.11)$$

The behavior of the scaling functions \mathcal{U} and \mathcal{V} when $r \rightarrow 0$ corresponds to taking $g = g_c$ at fixed j , hence we read off the expansions (7.4) of Z_j^c the following leading behaviors $\mathcal{U}(r) \sim 2/r^2$ and $\mathcal{V}(r) = -4(t + \frac{3}{2})/r^3$ (Q.) while $\mathcal{U}(r) \sim 3/r^2$ and $\mathcal{V}(r) = -6(t + 2)/r^3$ (E.T.). The functions \mathcal{U} and \mathcal{V} are further fixed by noting that $Z_j \rightarrow W = 2/(1 + \theta^2) = 2(1 - \theta^2 + O(\theta^4))$ at large j , hence $\mathcal{U}(r) \rightarrow 1$ and $\mathcal{V}(r) \rightarrow 0$ when $r \rightarrow \infty$. This results in [7]

$$\begin{aligned} \mathcal{U}(r) &= \frac{3}{\sinh^2\left(\sqrt{\frac{3}{2}}r\right)} + 1 & (\text{Q.}) \\ \mathcal{U}(r) &= \frac{3}{\sinh^2(r)} + 1 & (\text{E.T.}) \end{aligned} \quad (7.12)$$

while

$$\begin{aligned} \mathcal{V}(r) &= \left(t + \frac{3}{2}\right) \mathcal{U}'(r) & (\text{Q.}) \\ \mathcal{V}(r) &= (t + 2) \mathcal{U}'(r) & (\text{E.T.}) \end{aligned} \quad (7.13)$$

Expanding eqs.(7.12) and (7.13) above as power series of r , we have access to the θ expansion of Z_j of eq.(7.10) by writing $r = j\theta$, namely

$$\begin{aligned} Z_j &= 2 - \left(\frac{4}{j^2} - \frac{8}{j^3} \left(t + \frac{3}{2}\right) + O\left(\frac{1}{j^4}\right)\right) - \theta^4 \left(\frac{3}{5}j^2 + \frac{6}{5}j \left(t + \frac{3}{2}\right) + O(1)\right) \\ &\quad + \theta^6 \left(\frac{1}{7}j^4 + \frac{4}{7}j^3 \left(t + \frac{3}{2}\right) + O(j^2)\right) + \dots \\ Z_j &= 2 - \left(\frac{6}{j^2} - \frac{12}{j^3}(t + 2) + O\left(\frac{1}{j^4}\right)\right) - \theta^4 \left(\frac{2}{5}j^2 + \frac{4}{5}j(t + 2) + O(1)\right) \\ &\quad + \theta^6 \left(\frac{4}{63}j^4 + \frac{16}{63}j^3(t + 2) + O(j^2)\right) + \dots \end{aligned} \quad (7.14)$$

From the $\theta^6 = (1 - g/g_c)^{3/2}$ terms, we read off the singular parts of Z_j and $dZ_j/d\alpha_1$

$$\begin{aligned} Z_j|_{\text{sing}} &= \frac{j^4}{7} + O(j^3) & \frac{dZ_j}{d\alpha_1}|_{\text{sing}} &= \frac{4j^3}{7} \frac{dt}{d\alpha_1} + O(j^2) & \text{(Q.)} \\ Z_j|_{\text{sing}} &= \frac{4j^4}{63} + O(j^3) & \frac{dZ_j}{d\alpha_1}|_{\text{sing}} &= \frac{16j^3}{63} \frac{dt}{d\alpha_1} + O(j^2) & \text{(E.T.)} \end{aligned} \quad (7.15)$$

In particular, the leading contribution to $Z_j|_{\text{sing}}$ does not depend on the α 's and ρ 's. To evaluate $\langle m_j \rangle$ at large j , we now note that when all α 's and ρ 's are one, we have

$$\frac{Z_j(\{1; 1\})|_{\text{sing}}}{W_1(\{1; 1\})|_{\text{sing}}} = \sum_{l=1}^j \frac{\langle m_l \rangle}{\langle m_1 \rangle} \sim \begin{cases} \frac{3}{56}j^4 & \text{(Q.)} \\ \frac{2}{63}j^4 & \text{(E.T.)} \end{cases} \quad (7.16)$$

where we have used again the values of $W_1(\{1; 1\})|_{\text{sing}}$ above. The above result for quadrangulations is in agreement with that of Ref.[7] (eq.(4.19)). Using the above values of $\langle m_1 \rangle$, we therefore obtain by differentiating with respect to j :

$$\langle m_j \rangle \sim \begin{cases} \frac{6}{7}j^3 & \text{(Q.)} \\ \frac{8}{21}j^3 & \text{(E.T.)} \end{cases} \quad (7.17)$$

at large j . Gathering eqs. (7.8), (7.15) and (7.17), we finally deduce that $d\Gamma/d\alpha_1 = dt/d\alpha_1$ as announced.

7.3. Applications

As a first application of the above scheme, let us re-derive the results of Sections 4.1 and 4.2 for $k = 1$ with $\alpha_1 \equiv \alpha$ and $\rho_1 \equiv \rho$. Eqs.(3.12) reduce to $Z_1(1 - g\alpha(Z_1 + Z_2)) = \rho\alpha$ (Q.) and $Z_1(1 - g\alpha Z_2) = \rho\alpha$ (E.T.). Substituting $Z_1 = 2(t+1)(t+4)/((t+2)(t+3))$, $Z_2 = 2(t+2)(t+5)/((t+3)(t+4))$ and $g = 1/12$ (Q.) or $Z_1 = 2(t+1)(t+5)/((t+2)(t+4))$, $Z_2 = 2(t+2)(t+6)/((t+3)(t+5))$ and $g = 1/8$ (E.T.), we get the equations for t :

$$\begin{aligned} 6(t+1)(t+2)(t+4) - \alpha(2(t+1)(t^2 + 6t + 6) + 3\rho(t+2)^2(t+3)) &= 0 & \text{(Q.)} \\ 4(t+1)(t+3)(t+5) - \alpha(t+2)((t+1)(t+6) + 2\rho(t+3)(t+4)) &= 0 & \text{(E.T.)} \end{aligned} \quad (7.18)$$

with $t_0 = -1$ in both cases at $\alpha = 0$. We finally substitute $t = \Gamma - 1$ in eqs.(7.18) to recover eqs. (4.9) and (4.18).

To conclude this section, let us now display the algebraic equations as obtained via the above scheme for Γ in the case $k = 2$, with $\alpha_1 = \alpha$, $\alpha_2 = 1$, $\rho_1 = \rho$ and $\rho_2 = \sigma$. They read respectively for quadrangulations:

$$\begin{aligned}
& 6u^3\Gamma(u\Gamma + 4)(u\Gamma - u + 2)(u\Gamma + u + 2)(u\Gamma + 2u + 2) \\
& - \alpha \left(u^3\Gamma(u\Gamma + 4)(8 + 4u(2 + 3\Gamma) + 2u^2(3\Gamma^2 + 4\Gamma - 3) + u^3(\Gamma^3 + 2\Gamma^2 + 5\Gamma - 4) \right. \\
& \left. + 2u^4(\Gamma + 1)(3\Gamma + 1) + u^5\Gamma(\Gamma + 1)^2) + 3\rho(u\Gamma + 2)(u\Gamma - u + 2)^2(u\Gamma + 2u + 2)^2 \right) = 0
\end{aligned} \tag{7.19}$$

with $u = \sqrt{4 - 3\sigma}$, and for Eulerian triangulations:

$$\begin{aligned}
& 192\Gamma(\Gamma + u)(2\Gamma + u - 1)(2\Gamma + u + 3) \\
& - \alpha(2\Gamma + u - 3)(2\Gamma + u + 5) \left(48\Gamma(\Gamma + u) + \rho(u^2 - 1)(2\Gamma + u + 1)(2\Gamma + u - 1) \right) = 0
\end{aligned} \tag{7.20}$$

with $u = \sqrt{(27 - 2\sigma)/(3 - 2\sigma)}$. Again these equations are supplemented by the condition that $\Gamma = 1$ when $\alpha = \rho = \sigma = 1$ or alternatively that $\Gamma = 0$ when $\alpha = 0$.

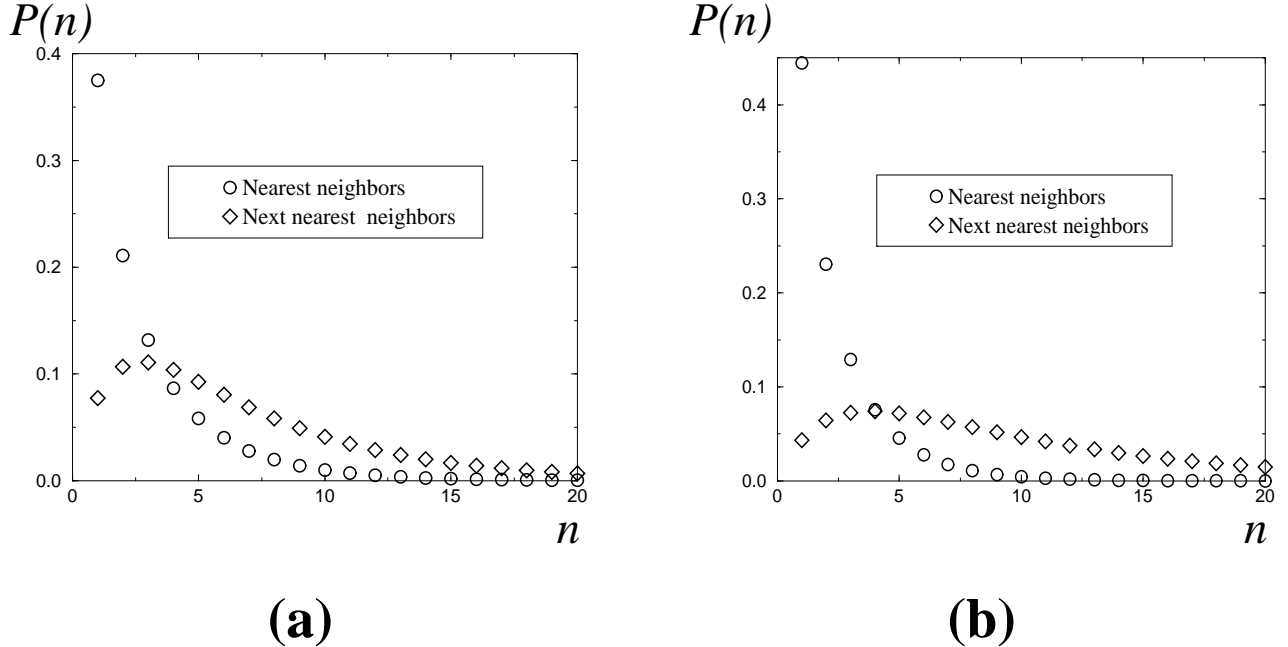


Fig.15: The probabilities $P(n)$ of having n nearest (resp. next nearest) neighboring vertices in infinite quadrangulation (a) and Eulerian triangulations (b), for $n = 1, 2, \dots, 20$. We note a maximum probability reached in the case of next nearest neighbors at $n = 3$ for quadrangulations and $n = 4$ for Eulerian triangulations, while the probabilities for nearest neighbors are strictly decreasing.

These equations allow to obtain various moments and probabilities involving next nearest neighboring vertices in infinite quadrangulations or Eulerian triangulations. For instance, we obtain the following first few moments of the numbers of next nearest neighboring vertices of the origin:

$$\begin{aligned} \langle n_2 \rangle &= \frac{54}{5}, & \langle n_2^2 \rangle &= \frac{24948}{125}, & \langle n_2^3 \rangle &= \frac{17067888}{3125} & (\text{Q.}) \\ \langle n_2 \rangle &= \frac{36}{5}, & \langle n_2^2 \rangle &= \frac{2148}{25}, & \langle n_2^3 \rangle &= \frac{4668948}{3125} & (\text{E.T.}) \end{aligned} \tag{7.21}$$

The probabilities $P(n)$ of having n next nearest neighboring vertices are displayed in Fig.15 (a) for quadrangulations and (b) for Eulerian triangulations, and compared with the corresponding probabilities for nearest neighbors as given by eqs.(5.2) and (5.6).

8. Conclusion

A completely open question regards the generalization to other graphs than quadrangulations and Eulerian triangulations. In Ref.[7], we have investigated a number of possible generalizations, either by allowing for faces with higher valences or by considering colored graphs, all of which turn out to have generating functions governed by discrete “integrable” recursion relations on the (suitably defined) geodesic distance, and for which compact “soliton-like” expressions also exist. These were derived by use of a somewhat different class of bijections between the duals of these graphs and some classes of so-called blossom trees with *constrained* valences [11,7]. To imitate the approach of the present paper, one would first need to derive a bijection involving geodesic distances, and with appropriately labeled trees with arbitrary valences, a task not performed yet. Another more promising approach would consist in adapting the techniques of the present paper directly in the language of blossom trees. For quadrangulations and Eulerian triangulations, both described by *binary* blossom trees with buds and leaves (see Refs.[11,12] for details), this involves weighting leaves, vertices and edges with suitable weights ρ_i (per leaf at the right of a face at depth i in the dual of the original graph), g (per vertex), and α_j (per edge bordering a face of depth j in the original graph). Repeating this weighting procedure in more general cases of blossom trees should give access to the local environment in so-called constellations, for instance two-constellations, i.e. graphs with arbitrary even-sided faces, which generalize quadrangulations, or three-constellations, which generalize Eulerian triangulations by allowing white faces with valences multiple of 3. Presumably, the

generalization of the blossom-tree construction proposed in Ref.[13] for arbitrary planar graphs should also allow to explore the local environment of a vertex as well.

Acknowledgments: We thank I. Kostov for pointing out Ref.[8]. All authors acknowledge support by the EU network on “Discrete Random Geometry”, grant HPRN-CT-1999-00161.

References

- [1] W. Tutte, *A Census of Planar Maps*, Canad. Jour. of Math. **15** (1963) 249-271.
- [2] E. Brézin, C. Itzykson, G. Parisi and J.-B. Zuber, *Planar Diagrams*, Comm. Math. Phys. **59** (1978) 35-51.
- [3] P. Di Francesco, P. Ginsparg and J. Zinn-Justin, *2D Gravity and Random Matrices*, Physics Reports **254** (1995) 1-131.
- [4] B. Eynard, *Random Matrices*, Saclay Lecture Notes (2000), available at http://www-spht.cea.fr/lectures_notes.shtml
- [5] G. Schaeffer, *Conjugaison d'arbres et cartes combinatoires aléatoires* PhD Thesis, Université Bordeaux I (1998).
- [6] P. Chassaing and G. Schaeffer, *Random Planar Lattices and Integrated SuperBrownian Excursion*, preprint (2002), to appear in Probability Theory and Related Fields, math.CO/0205226.
- [7] J. Bouttier, P. Di Francesco and E. Guitter, *Geodesic distance in planar graphs*, to appear in Nucl. Phys. B, cond-mat/0303272.
- [8] C. Godrèche, I. Kostov and I. Yekutieli, *Topological Correlations in Cellular Structures and Planar Graph Theory*, Phys.Rev.Lett. **69** (1992) 2674-2677; see also D. Boulatov, V. Kazakov, I. Kostov and A. Migdal, *Analytical and Numerical Study of a Model of Dynamically Triangulated Random Surfaces*, Nucl. Phys. **B275** (1986) 641-686.
- [9] P. Di Francesco, B. Eynard and E. Guitter, *Coloring Random Triangulations*, Nucl. Phys. **B516** [FS] (1998) 543-587.
- [10] J. Bouttier, P. Di Francesco and E. Guitter, *Random trees between two wall: Exact partition function* Saclay preprint T/03-086 (2003), cond-mat/0306602.
- [11] G. Schaeffer, *Bijective census and random generation of Eulerian planar maps*, Electronic Journal of Combinatorics, vol. **4** (1997) R20; see also G. Schaeffer, *Conjugaison d'arbres et cartes combinatoires aléatoires* PhD Thesis, Université Bordeaux I (1998).
- [12] M. Bousquet-Mélou and G. Schaeffer, *Enumeration of planar constellations*, Adv. in Applied Math., **24** (2000) 337-368; see also D. Poulalhon and G. Schaeffer, *A note on bipartite Eulerian planar maps*, preprint (2002), <http://www.loria.fr/~schaeffe/> and J. Bouttier, P. Di Francesco and E. Guitter, *Counting colored Random Triangulations*, Nucl.Phys. **B641** (2002) 519-532.
- [13] J. Bouttier, P. Di Francesco and E. Guitter, *Census of planar maps: from the one-matrix model solution to a combinatorial proof*, Nucl. Phys. **B645**[PM] (2002) 477-499.